Geological Survey of Finland

Bulletin 315

Geology, geochemistry and mineralogy of two Archean nickel-copper deposits in Suomussalmi, eastern Finland

by Kari K. Kojonen

Geologinen tutkimuslaitos
Espoo 1981

Geological Survey of Finland, Bulletin 315

GEOLOGY, GEOCHEMISTRY AND MINERALOGY OF TWO ARCHEAN NICKEL-COPPER DEPOSITS IN SUOMUSSALMI, EASTERN FINLAND

by

KARI K. KOJONEN

with 24 figures and 19 tables in the text

GEOLOGINEN TUTKIMUSLAITOS

ESPOO 1981

Kojonen, Kari K., 1981. Geology, geochemistry and mineralogy of two Archean nickel-copper deposits in Suomussalmi, eastern Finland. *Geological Survey of Finland, Bulletin 315.* 58 pages, 24 figures and 19 tables.

In eastern Finland the Archean complex (older than 2500 Ma) consists of three types of granites and rocks of the greenstone-belt association: ultramafic sills and extrusions, mafic and felsic volcanites and tuffs, phyllites, black schists, mica schists, banded iron formations, quartzites and conglomerates.

Two Ni-Cu sulphide deposits are associated with the ultramafic-felsic parts of the greenstone belt rocks: Hietaharju and Peura-aho. On the basis of geochemical whole-rock analyses and petrographic evidence, the ultramafic rocks are considered as cumulates of basaltic extrusives. They show predominantly a tholeiitic, subalkalic trend. Some ultramafic and mafic rocks of komatiitic composition occur among the analysed samples. The MgO content of the ultramafic rocks is 26—27 wt. %, corresponding to peridotite. In the upper part of the layered sill or extrusion the composition becomes pyroxenitic with 17—19 wt. % MgO and gabbroic with 11 wt. % MgO. The felsic volcanites are rhyolitic.

The sulphide compositions with a Cu/(Cu + Ni) ratio of 0.33 at Hietaharju and a Cu/(Cu + Ni) ratio of 0.30 at Peura-aho are transitional between the values of komatiites and tholeiites. The calculated MgO content in host rock is about 20 wt. %. The platinum group elements concentrated in samples rich in chalcopyrite and pentlandite have Pt/(Pt + Pd) ratio of 0.255—0.283 between komatiites and tholeiites.

The major ore minerals are hexagonal and monoclinic pyrrhotite, pentlandite, violarite, chalcopyrite, pyrite and magnetite. Minor amounts of zincian chromite, ilmenite, hematite, troilite, mackinawite, cubanite, sphalerite and gersdorffite also occur. The accessory ore minerals are gold, altaite, merenskyite, tellurobismuthite and wehrlite. Lattice constants and microprobe analyses are given for most of the ore minerals.

The ore mineral parageneses and petrographic evidence suggest that the sulphides originate from high temperature sulphide-silicate liquids. Three ore types are recognised: 1) disseminated and network type, 2) breccia type and 3) massive pyrite-rich type. The primary dissemination of sulphides was upgraded and remobilised during serpentinisation, carbonatisation and tectonic movements. The massive pyrite-rich ore was formed by sulphurisation.

Key words: Economic geology, nickel, copper, sulphides, mineralogy, greenstone belt, ultramafic rocks, Archean, Suomussalmi, Finland.

Kari K. Kojonen, Department of Geology, University of Helsinki, P.O. Box 115, SF-00171 Helsinki 17, Finland

ISBN 951-690-138-7
ISSN 0367-522X

Vammala 1981, Vammalan Kirjapaino Oy

CONTENTS

INTRODUCTION

In autumn 1959 people living in the Suomussalmi area sent several pyritiferous ore samples to Exploration Dept. of the mining company Outokumpu Oy. Most of the samples contained pyrite and pyrrhotite along with minor pentlandite and chalcopyrite. In spring 1960 a farmer, Mr. Gunnar Moilanen, sent to Outokumpu Oy a massive pyrrhotite sample that contained 2.37 wt. % Ni and 1.10 wt. % Cu. This was the sample that triggered exploration.

In 1960—1963 exploration included geological mapping, electrical, magnetometric and gravimetric surveys and diamond drilling (Pehkonen 1963). An airborne geophysical survey was made over an area of about 1000 km^2. Groundborne electrical and magnetic measurements covered an area of 46 km^2 and gravimetric survey 10 km^2. Diamond drilling totalled 11834 m. As a result two Ni-Cu deposits were found: Hietaharju and Peuraaho. The subeconomic ore with 0.81 wt. % Ni and 0.58 wt. % Cu at Hietaharju was estimated at 450 000 t.

In 1969—70 some parts of the deposits were excavated for sampling, and an additional 2523 m were drilled, mainly in the Peuraaho deposit (Inkinen 1970 a, b). The estimates for subeconomic ore reserves were recalculated: Hietaharju 238 000 t with 0.86. wt. % Ni, 0.43 wt. % Cu, 8.5 wt. % S, 18.2 wt. % Fe and 0.05 wt. % Co; Peura-aho 260 000 t with 0.58 wt. % Ni, 0.20 wt. % Cu, 7.4 wt. S, 14.22 wt. % Fe and 0.04 wt. % Co.

The present work is the outcome of a suggestion by Drs. P. Rouhunkoski and A. Häkli, Exploration Dept. of Outokumpu Oy, in January 1975. The aim has been to study the geochemistry and mineralogy of the Ni-Cu mineralisations at Hietaharju and Peuraaho and to compare them with known volcanogenic Archean Ni occurrances elsewhere in the world.

In the first half of this century it was assumed that most magmatic Ni deposits in the world are plutonic and were formed through magmatic segregation and gravitational differentiation from immiscible silicate—sulphide—oxide liquids. Experimental work from the early studies of Vogt (1893, 1917) to the extensive works of Kullerud and his coworkers has prowed the existence of magmatic segregation and greatly augmented our knowledge of silicate—sulphide—oxide phase relations in ultramafic intrusions (Craig and Kullerud 1969, Kullerud *et al.* 1969, Naldrett 1969 and others).

In 1969 Viljoen and Viljoen (1969 a—d) published their description of the geology of the granite—greenstone terrain in Barberton Mountain Land, South Africa. Volcanogenic structures were found in the Komati River ultramafic rocks: pillow lavas, flow-top breccias and crystalline quench textures. Analogous textures were found in Australia during prospecting for Ni deposits. They were called »spinifex» textures after a grass species of similar appearance (Nesbitt 1971).

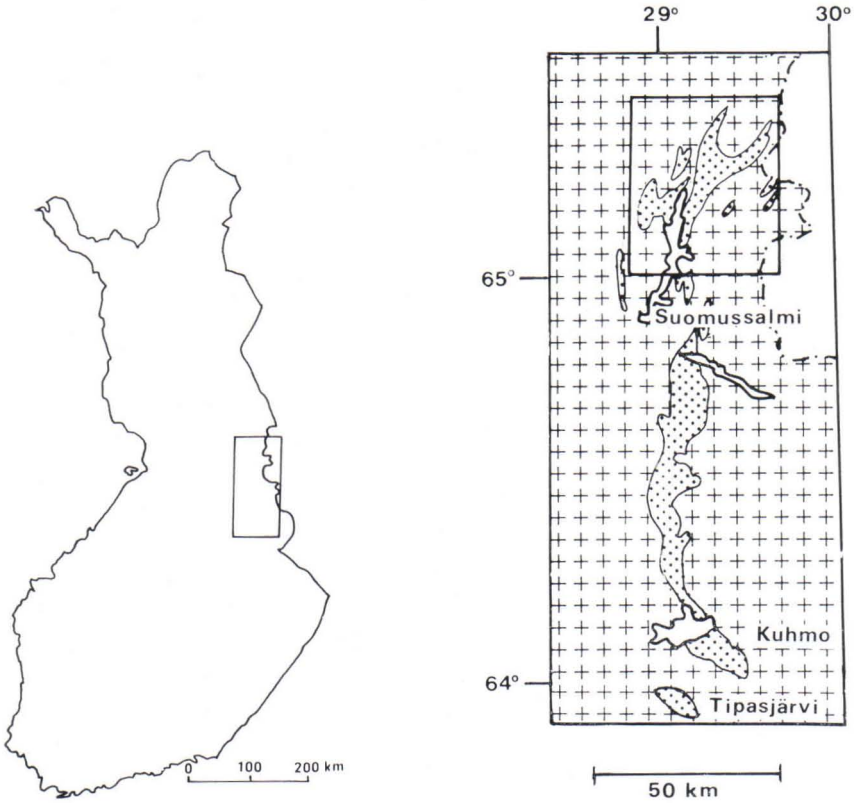

Fig. 1. The location of Suomussalmi, Kuhmo and Tipasjärvi greenstone belts (dotted) surrounded by granitoids (cross pattern), drawn after Simonen (1971).

Notable nickel discoveries in Western Australia in the late 1960's gave the incentive to exploration in other Precambrian shield areas (Knight 1975). The Archean volcanogenic rocks in the Precambrian shields have been subjected to extensive studies during the past ten years. Because of its association with large Ni-Cu deposits, the ultramafic part of the volcanogenic rocks proved to be economically very important.

Spinifex-textured ultramafic rocks were also found in many Canadian Ni deposits (Nalderett and Gasparrini 1971). Thus, the spinifex-textured ultramafic rocks, komatiites, acted as hosts of Ni deposits. Spinifex texture in peridotitic rocks is a diagnostic feature of komatiites, clearly indicating, that the rock is derived from very MgO-rich liquid with some mafic minerals. The absence of spinifex texture, however, does not necessarily imply that the rock is not komatiitic. The chemical composition of the rock plays a key role in the classification of basalts and nonspinifex ultramafic rocks in volcanogenic environment (Viljoen and Viljoen 1969 b, Arndt *et al.* 1977, 1979, Nesbitt *et al.* 1979).

Large Ni-Cu sulphide deposits have, however, also been found in the tholeiitic suites (Naldrett and Cabri 1976). In Pechenga, Kola Peninsula, in the U.S.S.R., the ultramafic and mafic rocks associated with the Ni-Cu de-

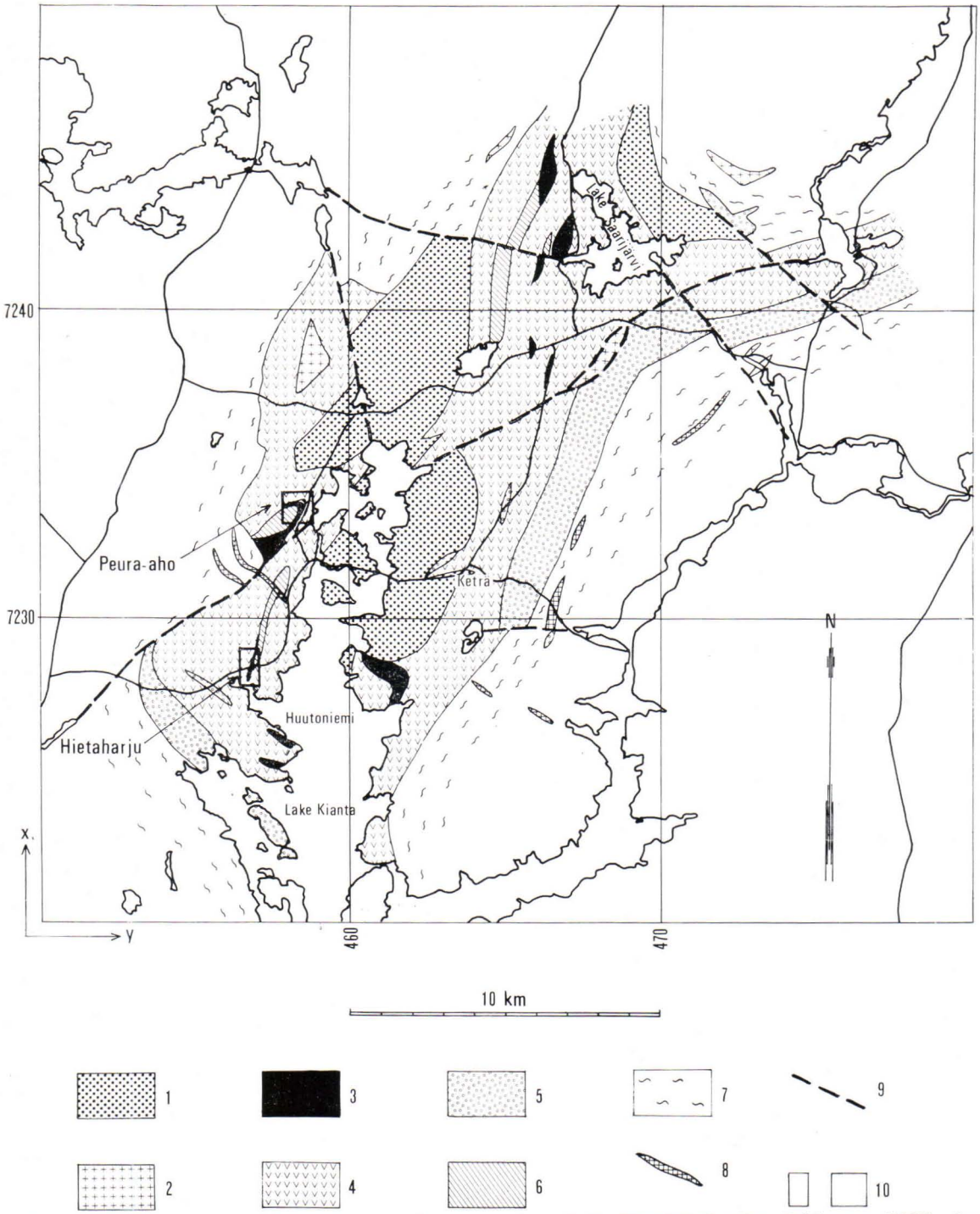

Fig. 2. Geological map of the Suomussalmi greenstone belt. Simplified after Pehkonen (1963). 1 = granodiorite; 2 = granite; 3 = ultramafic rocks; 4 = mafic volcanogenic rocks; 5 = arkosic quartzites 6 = felsic schists and porphyries; 7 = granite gneiss; 8 = diabases; 9 = major faults; 10 = Ni-Cu deposits.

posits are tholeiitic in composition. The ultramafic rocks of Pechenga have been classified as layered intrusions or layered sills (Väyrynen 1938, Haapala 1969, Naldrett and Cabri op.cit).

In northern Finland, the ultramafic rocks are of tholeiitic or komatiitic composition (Papunen *et al.* 1977, 1979).

In eastern Finland three Archean greenstone belts have been recognised: Suomussalmi, Kuhmo and Tipasjärvi (Fig. 1). The total length of these belts is about 150 km and the total width rarely exceeds 20 km. These belts may all be eroded remnants of the same greenstone belt formation. The komatiitic character of some of the mafic and ultramafic rocks in these belts was first proposed by Mutanen (1976). Blais *et al.* (1977, 1978) found two distinctive rocks series in these belts: komatiitic and tholeiitic. The Ni-Cu deposits described in the present paper are located in Suomussalmi greenstone belt and they are associated with metamorphosed ultramafic rocks, felsic porphyries and schists and black schists (Fig. 2).

SAMPLE MATERIAL

Samples were taken from diamond drill cores and ore outcrops. Altogether 128 polished and thin sections were prepared of the samples containing ore minerals. Most of the samples were duplicates of sulphide-rich cores already analysed for Cu, Ni, Co, Fe, S, Au, Ag, Pt and Pd during exploration in 1960—63 and 1969—70.

A total of 53 samples was collected for whole-rock analysis. The samples were taken from different rocks: 1) serpentinites and talc—carbonate rocks, 2) amphibole—chlorite rocks, 3) mafic volcanites, uralite porphyrites, mafic tuffs and amphibolites, 4) diabases, 5) felsic volcanites and porphyries, 6) granitoids and 7) argillaceous metasediments.

ANALYTICAL METHODS

Three types of chemical whole-rock analyses are given in this paper: 1) analyses made earlier by classical wet chemical methods (Wiik 1953, Matisto 1958), 2) analyses made by the author using the method described by Srivastava (1977), and 3) X-ray fluorescence (XRF) analyses performed at the Geological Laboratory of Outokumpu Oy.

The wet chemical analyses made by the author were carried out on a Perkin-Elmer 403 AAS unit. A group standard was prepared of Titrisol solutions and pure quartz. SiO_2, TiO_2 and P_2O_5 were measured colorimetrically on a Hitachi 101 spectrometer. Loss in ignition (LOI) was determined by annealing the finely powdered samples in platinum crucibles for 30 minutes at 1000°C.

For the XRF analysis the fine-powdered sample was mixed with plastic-cellulose (9:1) powder in a ratio 2:1 and pressed to pellets under 20 t weight. The pellets were analysed with a Philips PW 1310 X-ray analyser fitted

Table 1

Instruments and standards used in the microprobe analyses.

ARL EMX II, voltage 20 kV, current 15 μA, crystals LiF and ADP. Analyst, Dr. J. Ottemann.

Analysed mineral	Standard
Pyrrhotite	troilite
Pentlandite	millerite
Violarite	cobaltite
Chalcopyrite	chalcopyrite
Pyrite	pyrite, millerite, cobaltite
Sphalerite	sphalerite
Cubanite	chalcopyrite, troilite
Gersdorffite	millerite, cobaltite
Tellurobismuthite	metallic Bi and Te
Chromite	chromite, sphalerite
Magnetite	magnetite
Mackinawite	scanning pictures
Gold	scanning pictures

Geoscan Mark I, voltage 25 kV, current 10 μA, crystals LiF, mica and quartz. Analysts, Mrs. K. Hämäläinen, Mr. E. Hänninen and Mrs. M. Rannela.

Analysed mineral	Standard
Chromite	chromediopside, corundum,
Magnetite	eskolaite, Fe-Mn alloy,
Ilmenite	olivine, sphalerite
Gold	metallic Au and Ag
Wehrlite	metallic Te and Bi
Merenskylite	metallic Te, Bi, Pd, violarite
Gersdorffite	Ni- and Co-pentlandite, metallic As

with a Cr tube and using 60 kV and 30 mA, LiF and TlAP crystals in a vacuum of 10^{-1} Torr. The samples that the author analysed by wet methods were used as standards for the main elements. These samples range from peridotitic to rhyolitic. The trace elements were analysed with the aid of a gabbro-based trace-element standard mixed with plastic-cellulose powder. CO_2 was determined gravimetrically in samples leached with HCl. Graphitic C was analysed gravimetrically on the samples leached with acid after they had been heated in an induction owen.

The microprobe analyses were performed by Dr. J. Ottemann of the University of Heidelberg and by the staff of the Geological Laboratory of Outokumpu Oy. The instruments and standards used in the microprobe analyses are listed in Table 1. All the analyses were done on polished sections coated with graphite or aluminium.

A Philips PW 1051 X-ray diffractometer was used to produce the XRD charts of the powdered samples. Ni-filtered Cu-radiation with 35 kV and 15 mA was used especially for silicate minerals. In sulphide runs Mn-filtered Fe radiation with 30 kV and 9 mA was also used. The internal standards were Si and quartz. The lattice parameters were calculated with a programmable desk-top calculator.

The thin and polished sections were studied under a Leitz Ortholux microscope fitted with a Leitz MPV 1 photometer equipped with an interference graduated filter and a digital Fluke 8300 A voltameter output. The standards for the reflectance measurements were black glass N 2538.15 and carborundum No. 87, both obtained by courtesy of Dr. S.H.U. Bowie,[1] and tungsten carbide obtained by courtesy of Dr. N.F.M. Henry.[2]

The hardness (VHN) was measured on a Leitz Durimet according to the instructions of the Commission on Ore Microscopy (IMA).

[1] Commission on Ore Microscopy (IMA).
[2] Department of Mineralogy, University of Cambridge.

GENERAL GEOLOGY

The Archean bedrock in eastern Finland may be divided into rocks of the granitoid association and the greenstone belt association (Gaál *et al.* 1978).

The granitoid association includes three generations of granitoid rocks. The oldest generation is the granite gneiss or basement gneiss. It makes up the bulk of the bedrock in eastern Finland (Simonen 1971) and is thought to have been formed during ultrametamorphism from pre-existing supracrustal rocks or primordial ensialic crust, or both. The second and third generations are granodiorites and potassium granites and are considered to have been formed palingenetically.

The greenstone-belt association comprises volcanogenic rocks ranging from ultramafic to felsic, the dominant compositions being basaltic. Black schists, mica schists, phyllites and banded iron formations occur as intercalations in the mafic volcanics. Arenitic schists and polymictic conglomerates are deposited on top of the volcanics.

The diabase dykes in the area have been classified into two types: older diabases affected by orogeny and younger diabases crosscutting all other rock types in the area except the Iivaara ijolite massif (Matisto 1958).

Geochronologically, most of the rocks in eastern Finland are older than 2500 Ma (Kouvo 1958, Wetherill *et al.* 1962, Kouvo and Tilton 1966). Some of the volcanogenic rocks are obviously older than 3000 Ma; this is indicated by two Pb/Pb model ages of 3020 Ma and 3036 Ma from galena found in a felsic schist at Saarijärvi (M. Vaasjoki, pers. comm. 1979). The felsic schist is interbedded between granodiorite and ultramafic rocks and probably represents the closing stage of an early basaltic volcanic cycle (T. Kopperoinen, pers. comm. 1979).

The granitoid basement is thought to be older than 3000 Ma. The granodiorites are products of strong deformation, magmatism and ultrametamorphism that affected the basement gneiss 2700—3000 Ma ago. The youngest generation of granitoids, the potassium granite, is 2500–2700 Ma old. The granodiorites and granites have been intruded into the greenstone-belt volcanites and brecciated them. Thus, the greenstone belt deformed mainly between 2800 Ma and 3000 Ma ago (Gaál *et al.* 1978).

The structure of the Suomussalmi greenstone belt is disturbed by large faults (Fig. 2). The general strike of the foliation is NNE; the dip in the centre is very steep, becoming 40°—50° towards the margins of the greenstone belt. The axial plunge is usually 60°—70° NNE (Pehkonen 1963). Tectonic observations by Kokkola (1968) indicate intense isoclinal folding in the volcanogenic and sedimentogenic rocks of the greenstone-belt accociation.

The metamorphic grade of the mafic and ultramafic rocks in the Suomussalmi area is characterised by the following mineral assemblages:

(1) hornblende—albite—oligoclase—chlorite—epidote ± sphene,
(2) actinolite—albite—chlorite—epidote—sphene ± quartz,
(3) antigorite—talc—chlorite—carbonate ± actinolite ± epidote,
(4) talc—carbonate—chlorite—antigorite ± actinolite ± anthophyllite.

The first two assemblages of mafic rocks indicate low-grade metamorphism at high and low temperatures. They belong to the stability range of amfibolites and greenschists that are stable below 500°—550°C. The third

mineral composition indicates metamorphism of an ultramafic rock at low CO_2 pressures ($X_{CO_2} < 10$ %) and at temperatures below 480°C. The fourth assemblage reflects metamorphism at higher CO_2 pressures but at the same temperatures as in (3) (Winkler 1976, p. 151—199). The felsic schists and porphyries have the mineral composition:

(5) quartz—oligoclase—albite—biotite ± potassium feldspar ± chlorite ± muscovite ± sphene.

Staurolite and garnet occur sometimes in the felsic schists. Thus, depending on the pressure, the mineral assemblage indicates temperatures below 500—580°C (Winkler 1976, p. 204).

DESCRIPTION OF ROCK TYPES

The rock types in the Suomussalmi area have been described by Matisto (1958), Rantala (1963) and Kokkola (1968), whose reports are here only briefly cited.

Rocks of granitoid association

Granite gneiss

On a large scale this rock unit is fairly homogeneous; locally, however, there are inclusions of supracrustal rocks and plutonic bodies.

The granite gneiss around the Suomussalmi greenstone belt is mainly an oligoclase gneiss. It is often strongly lineated and gneissic in structure. Migmatitic features are common, and its colour varies from reddish to grey.

The major minerals are quartz, oligoclase and biotite. The minor and accessory minerals are microline, hornblende, apatite, epidote and opaque.

Granodiorites

The granodiorites have intruded into and brecciated the mafic volcanogenic rocks in the central part of the Suomussalmi greenstone belt. They are usually grey and slightly lineated.

The major minerals are plagioclase (An_{16-32}), biotite, hornblende and quartz. Minor minerals include microcline, epidote and chlorite. The accessories are zircon, muscovite, apatite, leucoxene and opaque.

Granites

The granites are homogeneous and nonfoliated. The major minerals are microcline, quartz and albite. Biotite is a minor constituent. The accessory minerals are apatite and opaque minerals. Muscovite and epidote are common alteration products.

Rocks of the greenstone belt association

Ultramafic rocks

The ultramafic rocks occur in two types: 1) serpentinites and 2) talc—carbonate rocks. The serpentinites are dark green, massive, fine- to coarse-grained rocks with a greyish green weathering surface. The rock is cut by thin veins of carbonate and talc. The major minerals are serpentine, tremolitic amphibole, chlorite, carbonate and talc. Pseudomorphs after olivine are common. Fine-grained opaque minerals, pyrrhotite, magnetite, pentlandite and chalcopyrite, are present in

Table 2

Chemical analyses in wt.% of rocks in the Suomussalmi greenstone belt.

	1	2	3	4	5	6	7	8	9	10	11	12	13
SiO_2	29.24	39.9	42.3	50.00	44.1	50.06	46.04	56.0	55.3	48.82	73.2	76.0	50.49
TiO_2	0.14	0.70	0.57	0.95	0.30	0.49	2.03	1.26	1.86	0.94	0.47	0.30	1.79
Al_2O_3	2.47	4.59	4.90	7.88	6.89	13.92	5.87	13.6	13.6	12.93	15.5	15.1	14.07
Fe_2O_3	6.53	—	—	—	—	—	1.75	—	—	—	—	—	2.27
FeO_{tot}	—	11.7	12.8	12.5	10.7	9.40	—	9.57	13.0	12.69	2.28	1.51	—
FeO	3.38	—	—	—	—	—	11.93	—	—	—	—	—	11.32
MnO	0.14	0.17	0.19	0.21	0.26	0.14	0.27	0.19	0.26	0.22	0.05	0.04	0.21
MgO	34.48	22.2	25.2	14.2	11.6	9.88	16.61	5.88	2.78	10.51	1.18	0.61	5.44
CaO	0.19	5.11	4.19	8.71	14.1	12.92	10.78	10.8	9.81	8.81	2.69	2.31	9.27
K_2O	0.13	0.02	0.00	0.14	0.03	0.08	0.15	0.15	0.16	0.12	2.48	0.95	0.82
Na_2O		0.38	0.78	0.28	0.00	1.75	0.16	1.24	1.27	1.63	0.45	1.63	2.64
P_2O_5	0.00	0.00	0.02	0.00	0.06	0.38	0.24	0.00	0.12	0.28	0.12	0.00	0.30
H_2O+	3.50	—	—	—	—	—	4.39	—	—	—	—	—	1.10
H_2O-	0.02	—	—	—	—	—	0.02	—	—	—	—	—	0.11
NiO	0.19	0.19	0.17	0.13	0.05	0.04	n.d.	0.01	0.12	0.02	0.00	0.01	n.d.
Cr_2O_3	0.31	0.33	0.54	0.27	0.20	0.14	n.d.	0.00	0.01	0.09	0.00	0.00	n.d.
LOI	—	11.7	8.34	4.48	9.19	n.d.	—	1.56	1.79	n.d.	2.55	2.20	—
CO_2	19.92	n.d.	n.d.	n.d.	n.d.	n.d.	n.d.	n.d.	n.d.	n.d.	n.d.	n.d.	n.d.
Total	100.64	96.99	100.0	99.75	97.48	99.20	100.24	100.26	100.07	97.06	100.97	100.66	99.83

n.d. = not determined
LOI = Loss of ignition

1. Talc–carbonate rock, Saarijärvi (Wiik 1953)
2. Talc–carbonate rock, Hietaharju. Analyst, K. Kojonen
3. Serpentinite, Peura-aho. Analyst, K. Kojonen
4. Amphibole–chlorite rock, Hietaharju. Analyst, K. Kojonen
5. Amphibole–chlorite rock, Peura-aho. Analyst, K. Kojonen
6. Coarse–grained amphibolite, Peura-aho, XRF analysis, Geological Laboratory, Outokumpu Oy
7. Greenstone, Saarijärvi (Matisto 1958)
8. Mafic volcanite, Hietaharju. Analyst, K. Kojonen
9. Mafic tuffite, sample Knm-1, 36.94. Analyst, K. Kojonen
10. Uralite porphyry, sample Knm-1, 17.04, XRF analysis, Geological Laboratory, Outokumpu Oy
11. Quartz–feldspar schist, Hietaharju. Analyst, K. Kojonen
12. Felsic porphyry, Peura-aho. Analyst, K. Kojonen
13. Diabase, Keträ (Matisto 1958)

small amounts. The serpentine is usually antigorite, but chrysotile has also been observed in some veins. The carbonate is mostly magnesite. An amphibole–chlorite rock consisting of tremolitic amphibole, chlorite and carbonate occurs in the contacts of the serpentinites. Foliation is pronounced.

The talc–carbonate rocks are yellowish grey, strongly schistose rocks with a network of carbonate veins. Rusty spots are frequently seen on the weathered surface. The carbonate is usually magnesite, but dolomite and ankerite are also present. Chlorite and amphibole occur in minor amounts. Quartz aggregates ranging from 5 cm to 25 cm in diameter and thin quartz veins are sometimes observed. There is also a zone of schistose amphibole–chlorite rock at the contacts of the talc–carbonate rocks.

The chemical composition (Table 2) of talc–carbonate rocks and serpentinites varies from dunitic to peridotitic. The amphibole–chlorite rocks are pyroxenitic.

Mafic rocks

Mafic volcanogenic rocks are most widespread in the Suomussalmi greenstone belt. This

group includes coarse-grained amphibolites, porphyritic and homogeneous lavas, pillow lavas, agglomerates, schistose greenstones and tuffs. Their colour varies from dark green to black. Amygdales consisting of calcite, quartz and epidote are common in the homogeneous lavas. Banding is clear in the mafic tuffs.

The chemical composition of the mafic volcanogenic rocks is usually basaltic (Table 2). The chemical analysis of the greenstone shows pyroxenitic composition.

The major minerals are hornblende, plagioclase and epidote. The amphibole is often altered into an actinolitic variety, chlorite and biotite. The plagioclase is zoned in the coarse-grained varieties: the core is An_{55} and the rim An_{10}. The small plagioclase grains are albite—oligoclase. The accessory minerals are sphene, leucoxene and opaque. The content of carbonate is often considerable in the greenstones.

The diabase veins usually strike E—W but strikes of N 40°—45° W are also common. The width of the veins varies from a couple of meters to tens of meters: the length is 200 to 400 m at the most. The colour is greenish black, and ophitic texture is distinct. The major minerals are uralitic amphibole and plagioclase. The lath-shaped plagioclase is zoned (An_{50-35}), becoming more albitic towards the rims. The accessory minerals are quartz, epidote, opaque and leucoxene. Biotite and chlorite occur as alteration products of amphibole.

Felsic rocks

Felsic schists and porphyries are associated with the ultramafic serpentinites and talc—carbonate rocks. The felsic schists gradually change to felsic porphyries. On weathered surface the colour varies from light grey to brown; on unweathered surfaces, it is darker bluish grey. Phenocrysts are occasionally recognisable in the porphyries. In chemical composition, the felsic schists and porphyries are rhyolitic (Table 2).

Microscopically, the porphyries are clearly porphyritic; the phenocrysts are quartz and andesine or oligoclase that is often cataclastic and zoned. The diameter of the phenocrysts is 0.5—3 mm. The matrix is very fine-grained and consists of albite, quartz, epidote, biotite, muscovite, carbonate, apatite and opaque. Secondary quartz veins are common.

Argillaceous metasediments

Mica schists, phyllites and black schists are interbedded in mafic and felsic volcanites and tuffs. The beds of argillaceous metasediments can usually be traced for several kilometres.

The major minerals are albite, quartz, biotite and muscovite. Epidote, chlorite, apatite, carbonate and hornblende occur as minor minerals. Appreciable sulphides and graphite are often present in the black schists. The grain size varies from coarse in the mica

Table 3

XRF analyses of argillaceous metasediments in the Suomussalmi area. The analyses are in wt.% recalculated to 100 % omitting volatiles. Analysed at Geological Laboratory, Outokumpu Oy.

	1	2	3	4
SiO_2	59.45	69.22	51.35	59.50
TiO_2	0.35	0.43	0.63	0.95
Al_2O_3	15.81	14.92	24.40	16.10
FeO_{tot}	6.59	6.10	10.74	12.34
MnO	0.11	0.03	0.17	0.19
MgO	7.25	3.55	5.73	4.60
CaO	6.07	0.06	1.21	2.91
Na_2O	2.42	0.24	2.42	2.78
K_2O	1.60	5.31	3.14	0.38
Cr_2O	0.07	0.06	0.11	0.17
P_2O_5	0.25	0.05	0.08	0.08
Total	99.97	99.97	99.98	100.00
S	0.00	0.00	0.00	3.51

1. Mica schist, x = 3012, y = 5640
2. Phyllite, x = 3700, y = 6609
3. Phyllite, x = 4279, y = 6612
4. Black schist, Peura-aho, average of 3 analyses.

schists to very fine in the phyllites and black schists.

The chemical analyses of argillaceous metasediments in the Suomussalmi area are given in Table 3. The argillaceous metasediments are weathering products formed during short periods of quiescence between the major volcanic episodes. The graphitic carbon presumably represents the remains of primitive organisms capable of living in a reducing environment (Rankama 1954). The graphitic carbon ranges in Peura-aho black schists from 0.3 to 7.2 wt. % (Huhma 1978). In the lake Saarijärvi area intercalations of banded iron formations have been observed in the phyllites.

Quartzites and conglomerates

In the eastern border area of the greenstone belt there is a bed of arkosic quartzite 1000—1500 m thick that also occurs on the western side of Lake Kianta about 2 km SW of the Hietaharju deposit and on the islands in the same lake. Conglomerates occur in the quartzites. The pebbles are polymictic, consisting of granite gneiss and volcanogenic rocks (Blais *et al.* 1977).

Table 4

Point-counting analyses of arkosic quartzite (Kokkola 1968).

	I	II	III	IV	V
Quartz	48.9	37.3	52.1	32.1	30.1
Plagioclase	25.1	32.6	30.4	44.7	47.9
Microcline	0.5	3.8	0.2	13.0	11.7
Biotite	3.2	1.7	5.9	3.0	3.0
Epidote	1.0	3.8	1.1	2.9	4.5
Chlorite / Muscovite	15.2	6.3	8.0	3.0	1.9
Others	6.1	14.5	2.3	1.3	0.9
Total	100.0	100.0	100.0	100.0	100.0

I—II Eastern bed
III—V Western bed

The medium-grained quartzites are light brownish grey. The major minerals are quartz and feldspars (Table 4). Biotite, carbonate, epidote, chlorite and muscovite are present in minor amounts. The accessory minerals are sphene, opaque and apatite. The texture is clearly clastic. Clasts of plagioclase 0.5—2 mm in diameter are common.

DESCRIPTION OF THE Ni-Cu DEPOSITS

The sulphide deposits of Hietaharju and Peura-aho are situated on the western shore of Lake Kianta (Fig. 2). Both deposits occur in an ultramafic rock associated with felsic schists and porphyries, black schists and mafic volcanites.

Hietaharju

The host rock of the sulphide ore bodies is an ultramafic lens consisting of talc—carbonate rocks, serpentinites and amphibole—chlorite rocks. The wall rocks are felsic schists to the east and mafic volcanites to the west (Fig. 3). The chemical analyses of the different rock types and of the ore bodies at Hietaharju are presented in Tables 5 and 6. Two types of ore have been established: 1) brecciating massive ore and 2) disseminated ore.

The massive ore consists (Fig. 4) of granular pyrrhotite, chalcopyrite and pentlandite that occurs in three shapes: 1) subhedral large grains, 2) interstitial bands between pyrrhotite grains and 3) exsolution »flames» within the pyrrhotite. Sphalerite, cubanite and

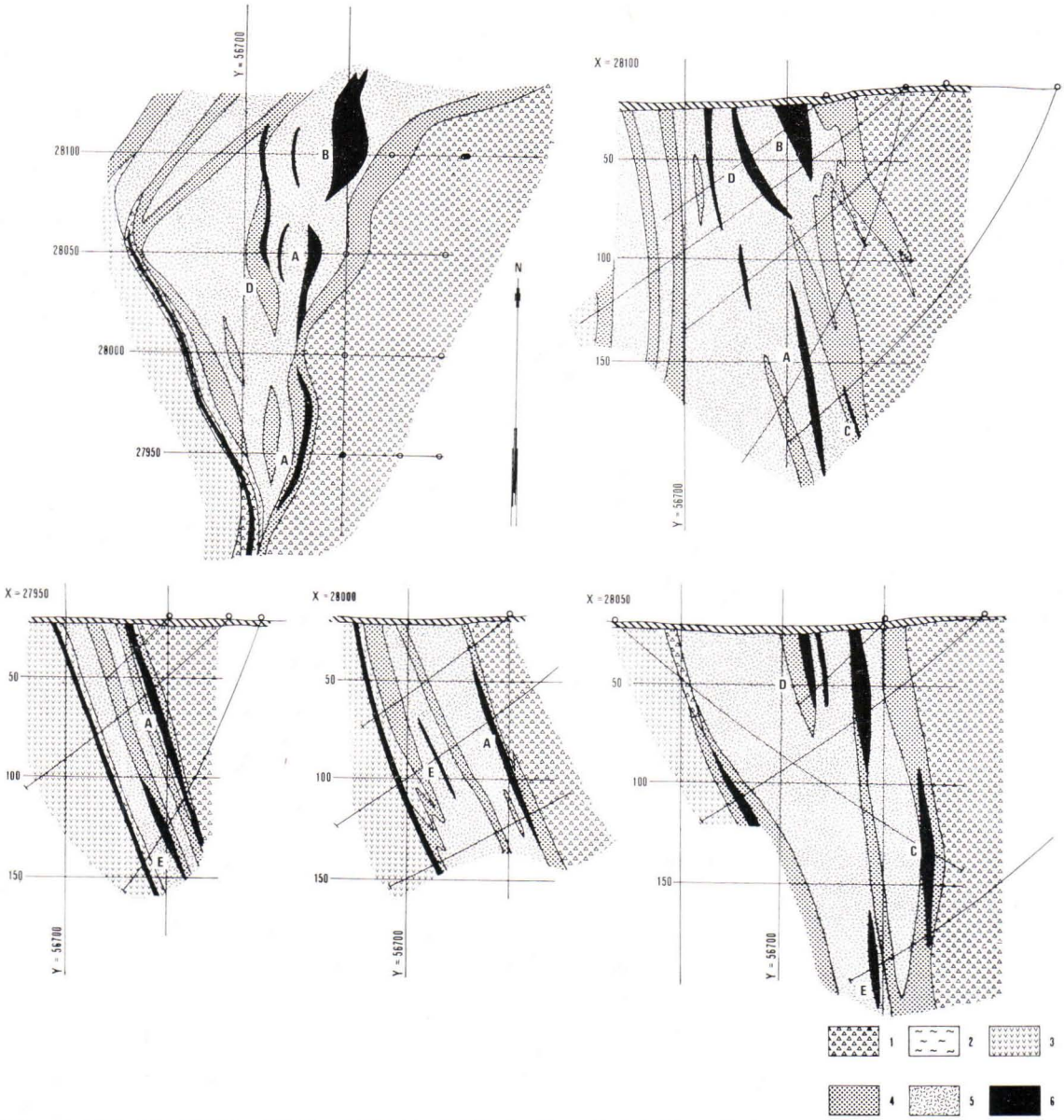

Fig. 3. The Hietaharju Ni-Cu deposit: surface plan (top left) and four cross sections simplified after Pehkonen (1963) and Inkinen (1970 a). 1 = felsic schist and porphyry; 2 = black schist; 3 = mafic volcanite; 4 = amphibole–chlorite rock; 5 = talc–carbonate rock and serpentinite; 6 = massive and disseminated ore. All numbers in the plan and cross sections are in meters.

mackinawite occur as inclusions in the chalcopyrite. There are numerous euhedral grains of magnetite containing drop-shaped inclusions of pyrrhotite, chalcopyrite and pentlandite. Ilmenite is sparse and occurs as separate grains or intergrown with magnetite. Some zoned chromites are also observed. In some samples gersdorffite—cobaltite is present as euhedral grains whose margins may be corroded (Fig. 5). Gold and tellurobis-

Table 5

Average XRF compositions of rocks in the Hietaharju deposit. The analyses were recalculated to 100 % omitting volatiles. Analysed at Geological Laboratory, Outokumpu Oy.

	1		2		3		4	
SiO_2 wt.%	47.56	(1.54)	48.37	(5.76)	55.74	(4.68)	70.53	(7.66)
TiO_2	0.48	(0.22)	0.84	(0.45)	0.69	(0.41)	0.41	(0.04)
Al_2O_3	6.74	(0.65)	8.14	(0.84)	13.72	(3.54)	19.12	(5.48)
FeO_{tot}	13.11	(0.37)	12.84	(1.00)	9.51	(1.21)	2.04	(0.35)
MnO	0.16	(0.11)	0.21	(0.09)	0.22	(0.03)	0.12	(0.03)
MgO	26.61	(1.46)	19.20	(2.94)	8.09	(2.72)	1.48	(0.29)
CaO	4.10	(1.39)	8.98	(0.41)	8.36	(7.05)	1.57	(1.03)
Na_2O	0.13	(0.08)	0.22	(0.21)	2.86	(2.46)	0.84	(0.61)
K_2O	0.06	(0.02)	0.07	(0.07)	0.23	(0.11)	3.47	(2.81)
Cr_2O_3	0.97	(0.10)	0.70	(0.18)	0.33	(0.21)	0.03	(0.01)
P_2O_5	0.11	(0.03)	0.23	(0.02)	0.26	(0.16)	0.11	(0.04)
Total wt.%	100.03		99.80		100.01		99.72	
CO_2 wt.%	4.28	(2.15)	2.33	(2.28)	0.93	(1.58)	0.73	(0.73)
S	0.30	(0.16)	0.16	(0.29)	0.71	(0.75)	0.42	(0.73)
As	0.00		0.01	(0.02)	0.00		0.00	
Ni ppm	2384	(556)	939	(148)	251	(101)	122	(165)
Cu	261	(176)	70	(112)	217	(217)	40	(19)
Zn	116	(26)	151	(20)	128	(29)	88	(35)
Pb	56	(22)	35	(11)	69	(19)	70	(70)
Ba	69	(79)	0		473	(320)	3088	(2059)
Sr	11	(6)	43	(34)	149	(92)	210	(173)
Rb	0		0		3	(2)	81	(49)
Zr	11	(1)	20	(5)	79	(60)	266	(63)
V	< 60		132	(18)	140	(57)	< 60	

Numbers in parentheses are standard deviations

1. Serpentinites and talc–carbonate rocks (4 analyses)
2. Amphibole–chlorite rocks (5 analyses)
3. Mafic volcanites (4 analyses)
4. Felsic schists (3 analyses)

Table 6

The average metal and sulphur contents in various ore bodies (A···D) in Hietaharju. Analysed at Outokumpu Oy (Inkinen 1970 a, b).

Ore body	Weight %					Cu/Ni	Cu / Cu + Ni	Pt / Pt + Pd
	Cu	Ni	Co	Fe	S			
A	0.53	0.84	0.06	18.9	8.5	0.63	0.39	0.333
B	0.43	0.94	0.05	19.0	8.5	0.46	0.31	0.286
C	0.35	0.93	0.06	18.7	9.6	0.38	0.27	0.231
D	0.23	0.58	0.03	11.1	4.9	0.40	0.28	—
Mean composition	0.43	0.86	0.05	18.2	8.5	0.50	0.33	0.283

muthite occur as inclusions in the gersdorffite.

In the disseminated ore the sulphides fill the interspaces between the gangue minerals. The ore-mineral paragenesis is essentially the same as in the massive ore but the arsenides are not present. The formation of zoned pyrite and marcasite as a result of weathering

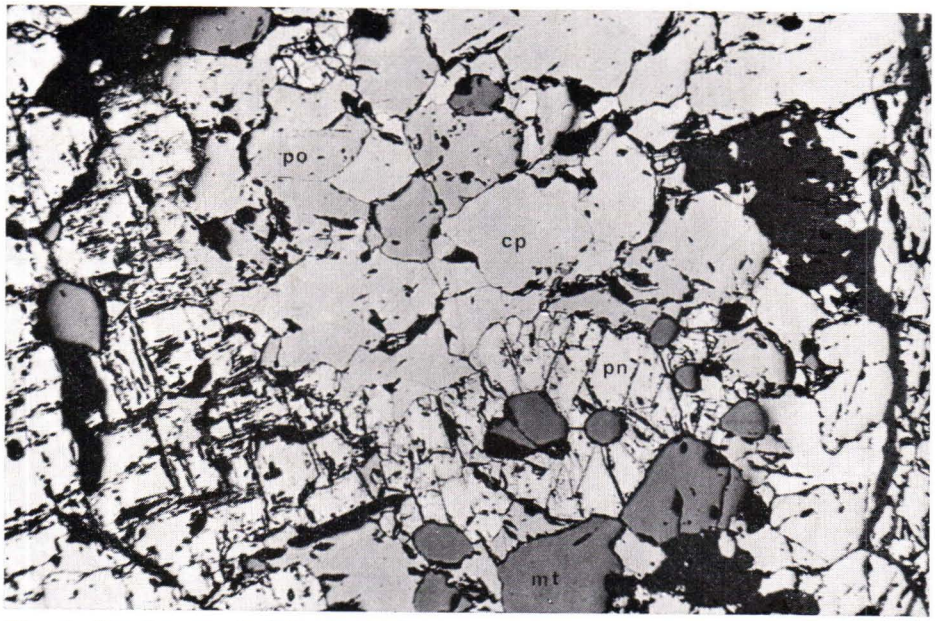

Fig. 4. Massive ore in talc-carbonate rock, Hietaharju A orebody, sample Sms H-7, 48.02 m, N //, 54 x, reflected light. po = pyrrhotite; cp = chalcopyrite; pn = pentlandite; mt = magnetite.

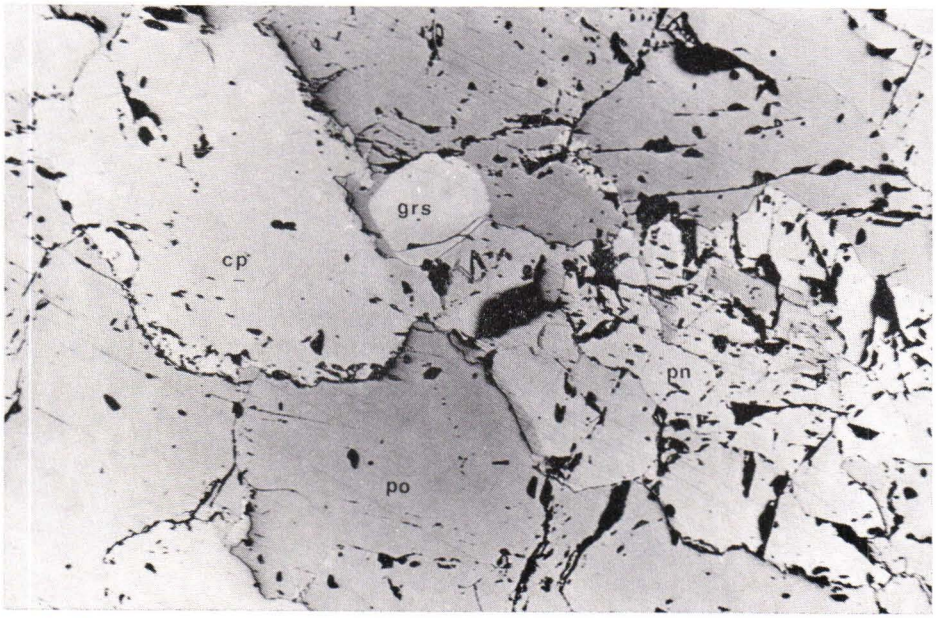

Fig. 5. Massive ore, Hietaharju C orebody, sample Sms-20, 185.08 m, N //, 54 x, reflected ligth. grs = gersdorffite.

is a common feature in both ore types. In some samples, pentlandite has altered completely into violarite.

The primary textures of the ultramafic rocks have been destroyed by metamorphism and tectonic movements. Foliation and microscopic isoclinal folding are visible in the thin sections made from diamond drill core samples.

The primary silicate minerals have altered into talc, carbonate, anthophyllitic and actinolitic amphibole, chlorite and minor serpentine. According to the XRD determinations, the carbonate is dolomite. The chlorite shows typical anomalous tobacco brown and indigo blue interference colours under crossed nicols. The diffractograms suggest that the chlorite belongs to the Mg-rich pennine series. Cummingtonitic amphibole, identified by XRD and optical methods, was found in one sample from the C ore body (see Fig. 3).

The talc—carbonate rocks and serpentinites grade into amphibole—chlorite rocks at the borders of the ultramafic lens and also inside the lens in places that possibly indicate shear zones. In the amphibole—chlorite rocks actinolitic amphibole forms radiating aggregates in a matrix consisting of chlorite plates 1—1.5 mm in diameter. In the fractures, the amphibole has altered into an olive green, fine-grained acicular mineral, probably iddingsite.

Most of the Ni ore bodies are situated near the eastern contact of the ultramafic lens with felsic schists. At the western contact, however, in a narrow zone of felsic schist, there is a zone of mainly iron sulphides that closely resembles those found in black schists elsewhere in the Suomussalmi area.

Peura-aho

The ultramafic host rock, serpentinite, is found in Peura-aho in the central part of an antiform whose axis plunges 100°/65°—75°. The outer part of the fold consists of thin beds of quartz—feldspar schist and black schist, which change to amphibole—chlorite rock, coarse-grained amphibolite and finally to mafic volcanite. The inner part of the fold is composed of a felsic quartz—feldspar schist, changing gradually to felsic porphyry with a zone of amphibole—chlorite rock between the felsic porphyry and the serpentinite (Fig. 6). The ore minerals occur as several lenses (A···E) in the antiform. Two ore types have been recognised: 1) massive pyrite-rich ore at the contact between felsic porphyry and amphibole—chlorite rock and 2) disseminated and vein network ore in the serpentinite.

The massive ore (B ore body in Fig. 6) consists mainly of pyrrhotite, pyrite, chalcopyrite and violarite (Fig. 7). Pyrite is subhedral or euhedral, containing inclusions of marcasite, chalcopyrite, pyrrhotite and magnetite. Chalcopyrite is granular with twinning lamellae. Pentlandite has mostly altered into violarite. Magnetite occurs as euhedral grains enclosing drop-shaped blebs of sulphides. Chromite and ilmenite are occasionally found as euhedral grains. In the weathered samples, pyrrhotite has altered into a dark brown »intermediate product» (Ramdohr 1969), marcasite.

The disseminated and vein-network ore (ore bodies A, D, E in Fig. 6) consists of disseminated oxide and sulphide ore minerals and veins of sulphides (Fig. 8). The oxides are zoned chromite with a magnetite rim, fine-grained magnetite and ilmenite. The sulphides in the disseminated ore are mostly penetrated by amphibole and serpentine formed during serpentinisation. The sulphides that consist mainly of pyrrhotite and pentlandite are situated chiefly between the pseudomorphs after olivine and pyroxene (Fig. 9). This proves that after the silicates had crystallised, the sulphides were still in liquid state.

The veins are filled with carbonate, talc

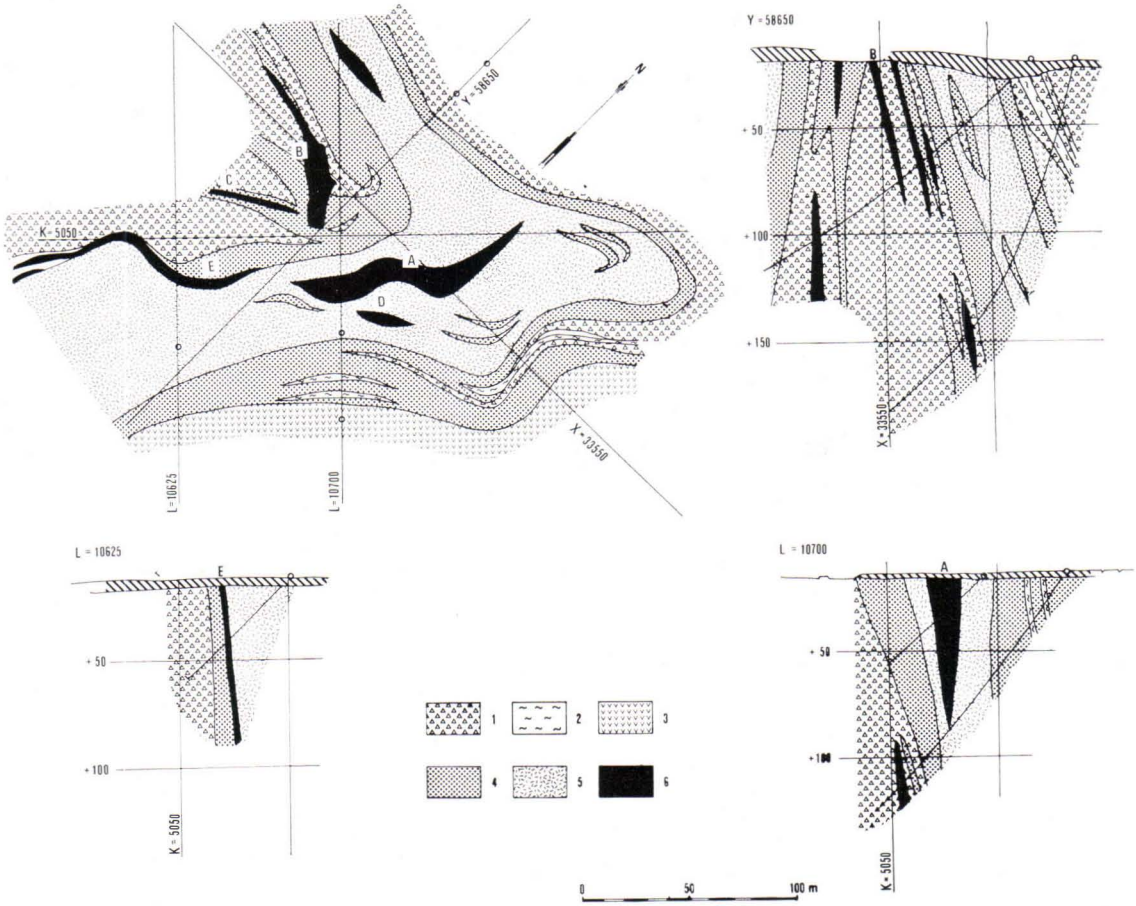

Fig. 6. The Peura-aho Ni-Cu deposit: surface plan (top left) and three cross sections simplified after Pehkonen (1963) and Inkinen (1970 a, b). The symbols are as in Fig. 3.

and sulphides. The major sulphides are pyrrhotite, chalcopyrite and pentlandite that occurs in three generations: 1) euhedral and subhedral grains, 2) interstitial bands between pyrrhotite grains and 3) »flame»-formed exsolutions in the pyrrhotite. Pentlandite has commonly altered into violarite. Chalcopyrite replaces euhedral pentlandite along the cleavage cracks. Pyrrhotite often shows signs of deformation as lamellar and platy grains. »Oleander leaf»- and lance-formed twinning is common in chalcopyrite.

Pyrite is present in small amounts as euhedral grains. In weathered samples pyrrhotite has altered into marcasite laths along the (0001) plane, into myrmekitic pyrite—magnetite intergrowths or into marcasite—pyrite »birds-eye» texture. Only a few grains of magnetite, hematite and ilmenite occur in the sulphide—carbonate veins. After solidification, the veins were cut by serpentine minerals (Fig. 8).

Microscopically the serpentinite consists of pseudomorphs after olivine or pyroxene (Fig. 9), which have altered into serpentine, chlorite and talc. The grain size of the pseudomorphs is 0.3—0.4 mm and in the matrix 0.05—0.1 mm. According to optical and XRD

Fig. 7. Photomicrograph of Peura-aho B orebody illustrating pyrite (py) euhedra in chalcopyrite (cp), altered pyrrhotite (po) and hematite-silica in the veins. Sample Sms PB-82, N //, 43 x, reflected light.

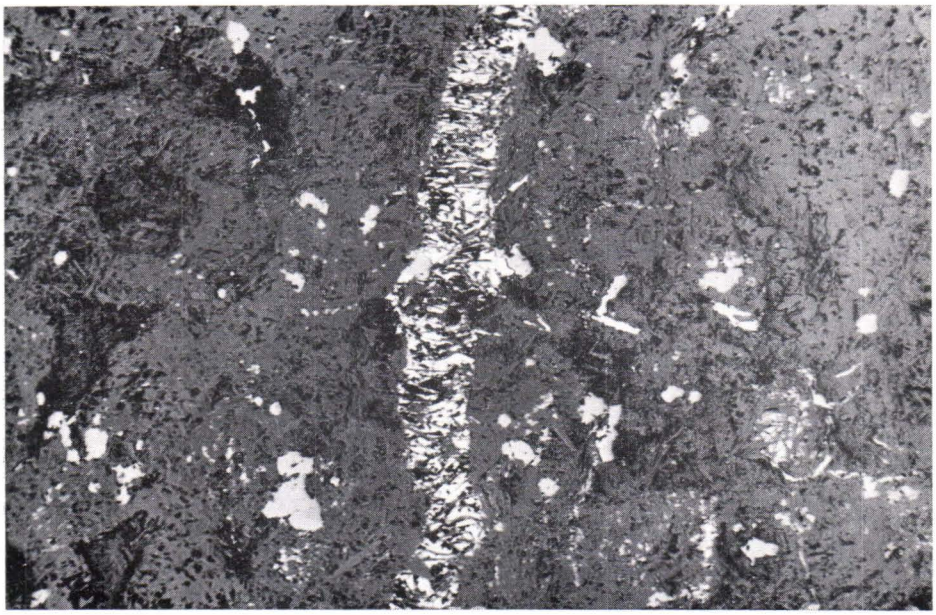

Fig. 8. Sulphide vein replaced by serpentinite minerals. Sample Sms P-7, 36.00 m, N //, 43 x, reflected light, Peura-aho A orebody.

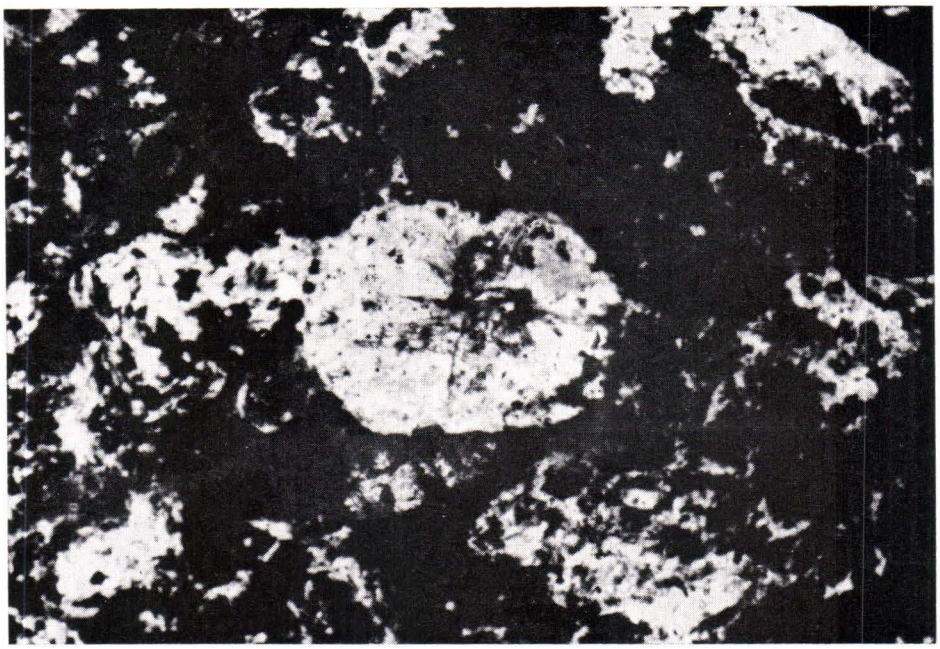

Fig. 9. Serpentine pseudomorph after olivine in a matrix of opaque. Sample Sms-1, 99.50 m, Peura-aho A orebody, N //, 32 x, transmitted light.

determinations the serpentine is antigorite. The chlorite is pennine. Together with carbonate minerals, usually dolomite—ankerite, talc occurs both in the matrix and in the veins. Also present are poikiloblastic grains of amphibole replaced by chlorite and serpentine. The amphibole is usually actinolitic although in the vicinity of felsic rocks it becomes edenitic or pargasitic, indicating slight sodium metasomatism. The minor minerals in the serpentinites are fine-grained epidote and leucoxene.

The amphibole—chlorite rocks are intensely foliated. They consist mainly of actinolitic amphibole phenocrysts, 0.5—1 mm in diameter, replaced poikiloblastically by chlorite and opaque and of a matrix containing fine-grained penninic chlorite and amphibole. The minor minerals are epidote, carbonate and opaque minerals enclosed in leucoxene.

The quartz—feldspar schist is clearly banded in thin section with coarse- and fine-grained bands and secondary quartz veins cutting the bands. The major minerals are quartz, oligoclase—albite, epidote, chlorite and biotite that is oriented parallel to the banding. Epidote and sphene occur as very fine-grained minerals throughout the rock.

The felsic schists change gradually to felsic quartz—feldspar porphyry with phenocrysts of twinned andesine and quartz and a matrix of fine-grained untwinned albite, chlorite, quartz, epidote and sphene. Cataclastic features are common in the phenocrysts.

The coarse-grained amphibolite in the upper part of the anticline consists of actinolitic amphibole phenocrysts, pseudomorphous after pyroxene and a fine-grained matrix composed of altered plagioclase, clinozoisite, chlorite, epidote and muscovite. The minor minerals are carbonate, sphene and opaque.

Study of the mineral composition of black schists is hampered by the very fine grain size. According to XRD determination on a

Table 7

Average XRF compositions of rocks in the Peura-aho deposit. The analyses were recalculated to 100 % omitting volatiles. Numbers in parentheses are standard deviations. Analysed at Geological Laboratory, Outokumpu Oy.

	1	2	3	4	5	6
SiO_2 wt.%	45.62 (0.95)	47.98 (4.64)	51.71 (1.50)	61.34 (3.20)	70.47 (7.35)	59.50 (7.90)
TiO_2	0.51 (0.09)	0.58 (0.24)	0.49 (0.08)	1.83 (1.44)	0.38 (0.09)	0.95 (0.79)
Al_2O_3	4.72 (0.61)	8.01 (2.22)	12.30 (2.09)	13.25 (1.58)	15.75 (1.67)	16.10 (4.49)
FeO_{tot}	14.45 (0.79)	15.64 (4.42)	9.81 (0.76)	10.91 (3.39)	3.53 (2.92)	12.34 (5.21)
MnO	0.33 (0.04)	0.28 (0.05)	0.14 (0.02)	0.29 (0.07)	0.15 (0.06)	0.19 (0.07)
MgO	27.76 (1.04)	17.52 (7.94)	11.09 (1.54)	3.72 (0.48)	1.74 (1.02)	4.60 (3.82)
CaO	4.85 (0.77)	8.50 (4.28)	11.86 (2.02)	3.95 (1.88)	3.39 (2.72)	2.91 (2.04)
Na_2O	0.37 (0.26)	0.37 (0.60)	1.84 (0.86)	2.34 (2.48)	3.21 (2.56)	2.78 (0.98)
K_2O	1.11 (0.05)	0.09 (0.09)	0.20 (0.09)	2.13 (0.91)	1.32 (0.38)	0.38 (0.36)
Cr_2O_3	1.16 (0.26)	0.66 (0.53)	0.19 (0.12)	0.08 (0.04)	0.08 (0.03)	0.17 (0.09)
P_2O_5	0.14 (0.02)	0.27 (0.17)	0.37 (0.05)	0.17 (0.07)	0.15 (0.14)	0.08 (0.05)
Total wt.%	100.02	99.90	100.00	100.01	100.17	100.00
CO_2 wt.%	3.18 (1.57)	2.05 (2.78)	n.d.	0.32 (0.32)	3.50 (2.26)	0.53 (0.84)
S	0.41 (0.32)	0.27 (0.46)	0.09 (0.16)	0.10 (0.05)	0.57 (0.57)	3.51 (4.11)
As	0.01 (0.03)	0.00	0.00	0.00	0.00	0.00
Ni ppm	1774 (449)	657 (498)	287 (89)	126 (26)	131 (69)	486 (94)
Cu	343 (214)	135 (243)	98 (55)	179 (108)	115 (76)	729 (94)
Zn	155 (67)	107 (24)	145 (22)	203 (66)	161 (137)	113 (23)
Pb	94 (11)	39 (14)	46 (18)	131 (52)	87 (48)	49 (21)
Ba	33 (46)	0	215 (126)	1079 (276)	918 (233)	313 (456)
Sr	18 (5)	28 (31)	181 (83)	332 (86)	302 (79)	162 (120)
Rb	2 (3)	0.5 (0.5)	3 (3)	62 (33)	32 (3)	9 (11)
Zr	14 (14)	25 (20)	36 (13)	114 (9)	104 (18)	76 (35)
V	133 (70)	170 (89)	n.d.	325 (169)	67 (12)	167 (31)

n.d. = not determined

1. Serpentinites (4 analyses)
2. Amphibole–chlorite rocks (6 analyses)
3. Coarse-grained amphibolites (5 analyses)
4. Hypabyssic rocks (4 analyses)
5. Felsic schists and porphyries (3 analyses)
6. Black schists (3 analyses)

Table 8

The average metal and sulphur contents in various ore bodies (A···E) in Peura-aho (Pehkonen 1963, Inkinen 1970 a, b).

Ore body	Weight %					Cu/Ni	Cu / Cu + Ni	Pt / Pt + Pd
	Cu	Ni	Co	Fe	S			
A	0.20	0.52	0.03	9.9	3.1	0.41	0.29	0.333
B	0.31	0.76	0.03	20.49	16.76	0.41	0.29	0.176
C	0.51	0.81	n.d.	n.d.	n.d.	0.62	0.39	—
D	0.13	0.35	0.03	7.7	1.4	0.37	0.27	—
E	0.14	0.44	0.05	18.8	8.4	0.33	0.25	—
Mean composition	0.2	0.58	0.04	14.22	7.4	0.43	0.30	0.255

powdered rock sample, the major minerals are quartz, albite, chlorite, pyrite, dolomite and graphite.

Hypabyssic rocks, called diabases in the reports of Pehkonen (1963) and Inkinen (1970 a, b), occur at Peura-aho and Hietaharju, although they do not show up in Figures 3 and 6. They behave both discordantly and concordantly. The major minerals are hornblende, plagioclase, biotite, epidote, carbonate and quartz. The hornblende and plagioclase (An_{30}) occur as laths up to 2 mm long. The accessory minerals are opaque and leucoxene. In weathered samples the hornblende is wholly altered into chlorite.

The chemical analyses of different ore and rock types are given in Tables 7 and 8.

GEOCHEMICAL RESULTS

The chemical whole-rock analyses of different rocks at Hietaharju and Peura-aho are given in variation diagrams in Figures 10—12. Middlemost (1975) divides basalts into alkalic, sub-alkalic low potassium, and sub-alkalic groups on the basis of the diagrams Na_2O vs. SiO_2 and K_2O vs. SiO_2. In these diagrams, the Suomussalmi rocks plot in the sub-alkalic low-potassium field (Fig. 10 a, b). In the $Na_2O + K_2O$ vs. SiO_2 diagram (Fig. 10 c), the Hietaharju and Peura-aho samples plot in the sub-alkalic field common for tholeiitic and komatiitic rocks (Viljoen and Viljoen 1969 b, Irvine and Baragar 1971). In the AFM diagram, (Fig. 10 e) the analysis points form a continuous rock series: I serpentinites and talc—carbonate rocks (peridotitic), II amphibole—chlorite rocks (pyroxenitic), III basaltic volcanites and tuffs and IV felsic schists and porphyries (dacitic and rhyolitic). Groups I and II plot in the tholeiitic field and group IV plots in the calc-alkaline field (Irvine and Baragar 1971). In the $CaO—MgO—Al_2O_3$ diagram (Fig. 10 d) most of the mafic rocks of Suomussalmi plot in the fields of basaltic picrites and of oceanic or continental tholeiites. Only a few of the samples lie in the komatiite fields (Viljoen and Viljoen 1969 b). The komatiites and tholeiites were separated by Naldrett and Cabri (1976) and Arndt *et al.* (1977) using the Al_2O_3 vs. $FeO/(FeO + MgO)$ plot. In this diagram (Fig. 11 a), more than half of the analysed rocks are situated below the dividing line in the tholeiitic field. According to the definition proposed by Brooks and Hart (1974) for basaltic komatiite, the TiO_2 content has to be less than 0.9 wt.%. The plot TiO_2 vs. SiO_2 (Fig. 11 b) shows that most of the Suomussalmi samples satisfy this constraint. A third of the samples, however, show a TiO_2 content exceeding 0.9 %. The CaO/Al_2O_3 ratio more than 1 was also included in the original definitions of Viljoen and Viljoen (1969 b) and Brooks and Hart (1974). In this respect, some of the analysed rocks (Tables 5 and 7) may be classified as komatiites. In the diagrams Ni vs. MgO and Cr vs. MgO (Fig. 11 d, e), the same four groups can be identified as in the AFM diagram. The highest Ni and Cr contents occur in peridotitic samples. The distribution of Cu is more random (Fig. 11 c). Anomalous Cu contents occur in the black schists and in some pyroxenitic and peridotitic rocks. The Zn and Pb contents are low (50—200 ppm) in all the samples. In the plots of Zr, Ba, Sr, Rb vs. MgO (Fig. 12 a—d) the increase in contents with decreasing MgO is evident. The Zr, Ba, Rb and Sr contents are somewhat higher than those in the komatiitic and tholeiitic

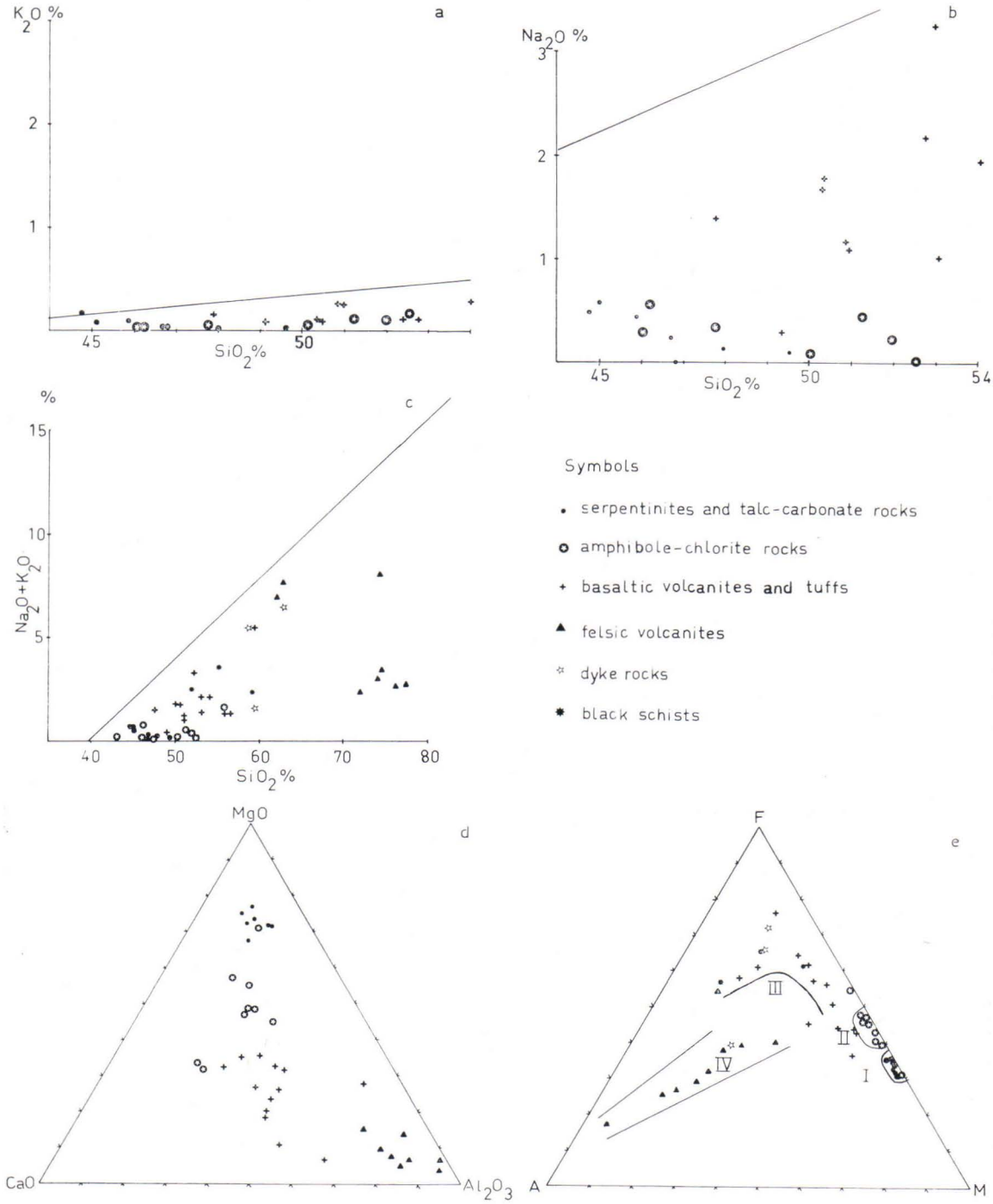

Fig. 10. Na_2O-K_2O vs. SiO_2, AFM and MgO-CaO-Al_2O_3 diagrams of the analysed samples.

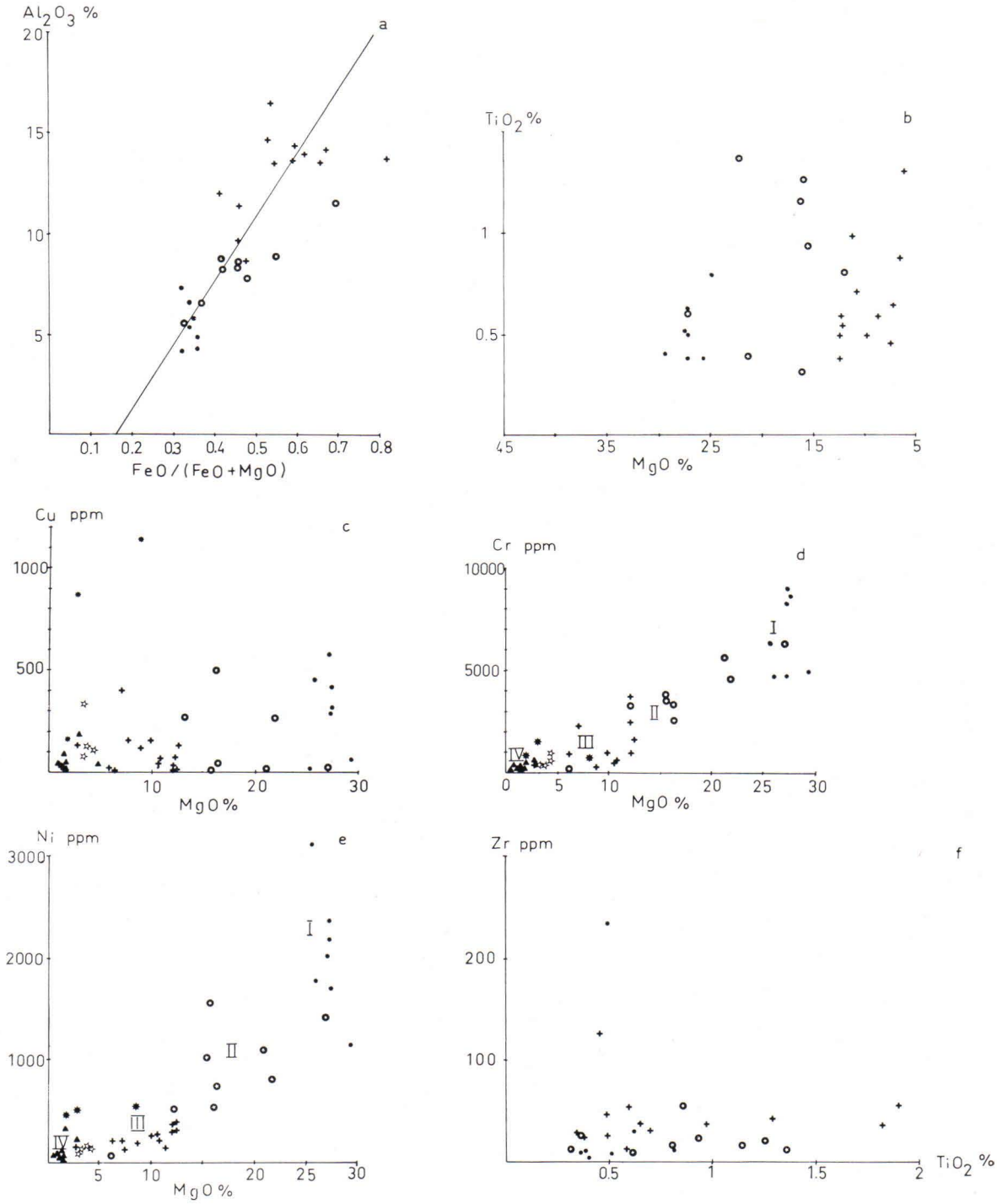

Fig. 11. Al_2O_3 vs. FeO/(FeO + MgO), TiO_2, Cu, Cr, Ni vs. MgO and Zr vs. TiO_2 diagrams of the analysed samples.

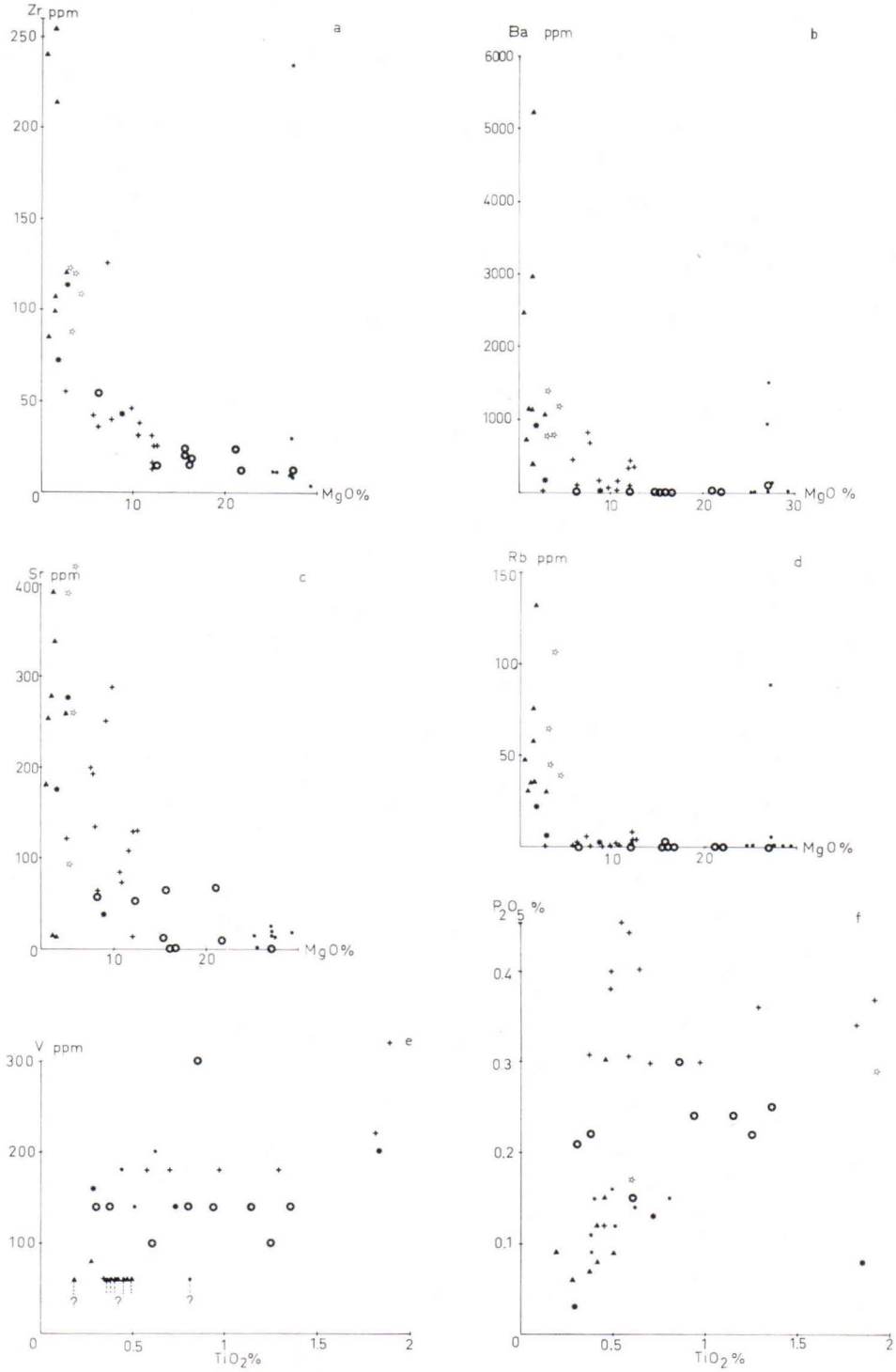

Fig. 12. Zr-Ba-Sr-Rb vs. MgO and V-P_2O_5 vs. TiO_2 diagrams of the analysed samples.

peridotites and basalts in Canada, South Africa and Western Australia (Nesbitt and Sun 1976, Arth *et al.* 1977). Further evidence of contamination is provided by some anomalously high Zr, Ba and Rb contents in peridotitic samples. The contamination could have taken place either when the basaltic magma extruded through the sialic crust or later when the granodioritic material intruded as dykes. In the Zr vs. Ti diagram (Fig. 11 f), Nesbitt and Sun (1976) found a chondritic trend for komatiites and tholeiites in Canada, South Africa and Australia. No such trend has been observed in the Suomussalmi samples; on the contrary, anomalously high Zr contents existed on some samples. In the V vs. TiO_2 diagram (Fig. 12 e) one half of the samples plots in the field of spinifex-textured peridotites; the other half has tholeiitic contents of these elements. The P_2O_5 content for komatiites are usually very low (0.02—0.04 wt.%). The analysed P_2O_5 contents plotted in the P_2O_5 vs. TiO_2 diagram (Fig. 12 f) of the Suomussalmi samples exceed mostly 0.1 %, as is typical of tholeiitic series.

At Peura-aho the analytical data indicate magmatic layering: on the bottom there is a peridotitic serpentinite (average MgO content 27.76 wt.%) that grades from pyroxenitic amphibole—chlorite rock (average MgO content 17.52 wt.%) into coarse-grained magnesian basaltic amphibolite (average MgO content 11.09 wt.%) and finally into basalt.

At Hietaharju the layering is not so clear as at Peura-aho. In the western margin of the ultramafic lens there is, however, a zone of amphibolite 4 to 8 m thick that indicates the top of the lens (Inkinen 1970 a). At Hietaharju, the talc—carbonate rocks are peridotites (average MgO content 26.61 wt.%) and grade into pyroxenitic amphibole—chlorite rocks, which in turn change to amphibolites and finally to basalts (average MgO content 8.36 wt.%). At Hietaharju the ultramafic lens seems to rest on the felsic schist (Fig. 13 b). The schistosity of the amphibole—chlorite rocks and felsic schist is a product of deformation, that took place either at the extrusive stage as a result of flow or during later tectonic movements.

Komatiitic host rock compositions have been observed in both deposits. Indisputable spinifex textures have not been found in these rocks, which otherwise might be komatiites according to the definition of Brooks and Hart (1974). The cumulate texture observed in several samples of the Peura-aho serpentine shows that the temperatures of the original melts were not so high as those of the komatiitic lavas (Green *et al.* 1975). The chemical compositions are, however, predominantly tholeiitic. Thus, the most logical mode of origin of the Suomussalmi ultramafic rocks seems to be a layered basal accumulation of tholeiitic basaltic magmas.

In both deposits carbonatisation and hydration have changed the original mineral parageneses of the ultramafic rocks (Winkler 1976, p. 153):

(1) 2 forsterite + 2 H_2O + 1 CO_2 ⇌ 1 serpentine + 1 magnesite;

(2) 4 forsterite + 2 H_2O + 5 CO_2 ⇌ 1 talc + 5 magnesite;

(3) 2 serpentine + 3 CO_2 ⇌ 1 talc + 3 magnesite + 3 H_2O.

The talc—carbonate association indicates a higher CO_2 pressure than does the serpentine—chlorite—talc association. This is shown by the average CO_2 contents determined: 4.28 wt.% in Hietaharju talc—carbonate rock and 3.18 wt.% in Peura-aho serpentinites (Tables 5 and 7).

To avoid the effect of variation in volatiles the XRF analyses made at the Geological Laboratory of Outokumpu Oy were recalculated by the author on a volatile-free basis to 100 %. The recalculation does not seem to affect the rock composition; rather, it reveals the primary composition before metamorphism (Muir 1979).

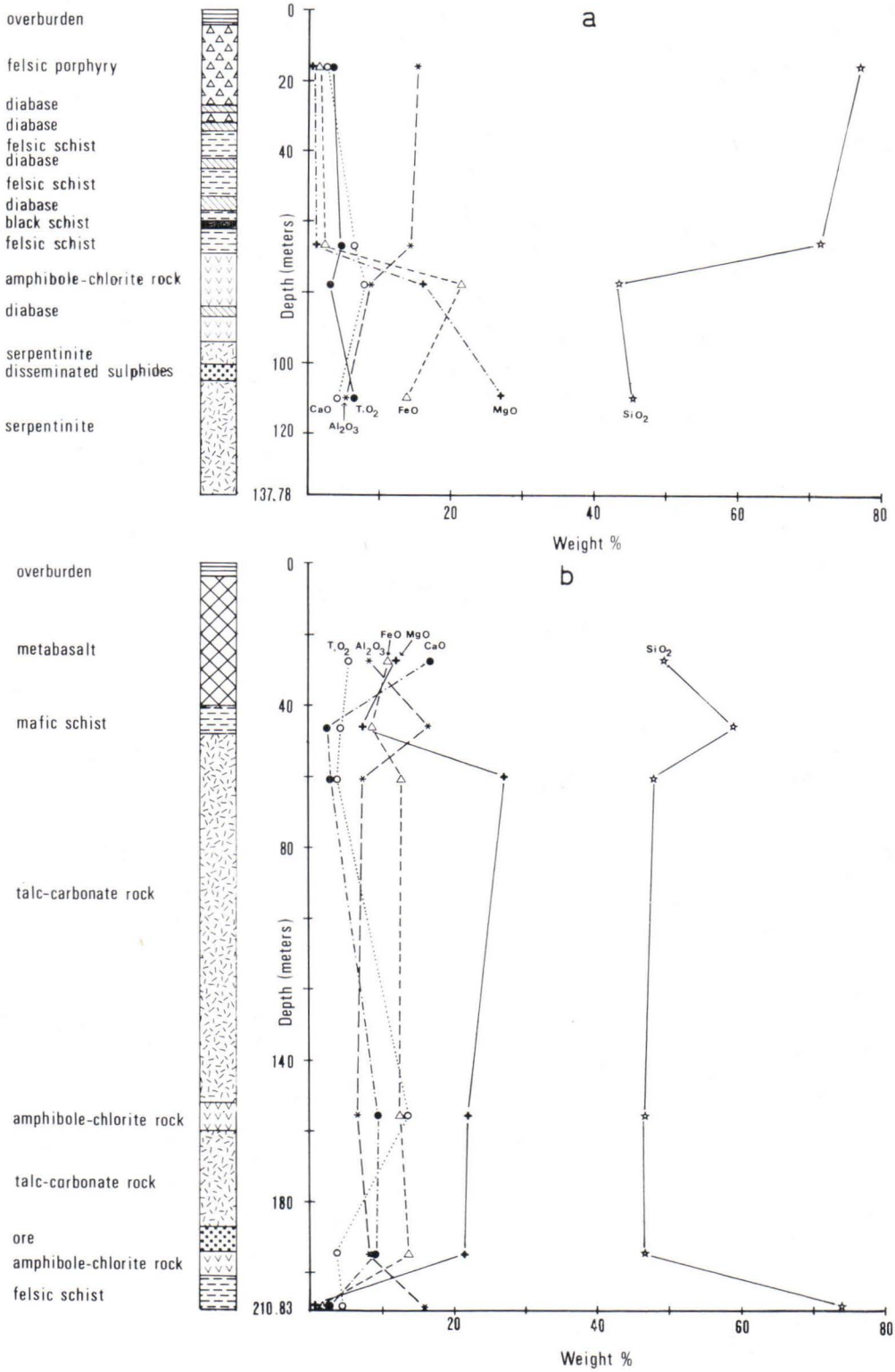

Fig. 13. Two diamond drill core profiles of the Suomussalmi Ni-Cu deposits: a) Sms-1, Peura-aho; b) Sms-20, Hietaharju. The TiO_2 contents are exaggerated ten times in the diagrams.

SULPHIDE ORE ANALYSES

The classification of ultramafic and mafic rocks by Naldrett and Cabri (1976) was based on diagrams of the ratios Cu/(Cu + Ni) vs. MgO and Pt/(Pt + Pd) vs. Cu/(Cu + Ni). The analytical data of the Suomussalmi sulphide ore bodies given in Tables 6 and 8 are plotted in these diagrams (Fig. 14). The MgO percentage of the host rock was calculated as an average for the talc—carbonate rocks, serpentinites and amphibole—chlorite rocks. Platinum-group elements occur mainly in massive chalcopyrite- and pentlandite-rich samples that usually contain some arsenides. In the upper diagram (Fig. 14), the Suomussalmi samples plot between komatiites and tholeiites. The Pt/(Pt + Pd) ratio decreases with increasing differentiation and thus indicates that the Suomussalmi ultramafic rocks are more differentiated than the komatiites and also more differentiated than the tholeiites of Pechenga and Sudbury. The Cu/Ni ratio has, however, a common increasing trend with decreasing maficity of the host rock (Naldrett and Cabri 1976). Thus, the Suomussalmi rocks are less mafic than the komatiites but approximately as mafic as the tholeiites of Pechenga.

In the lower diagram the Suomussalmi samples are located between the composition bars of Abitibi and Pechenga. According to Naldrett and Cabri (1976), the Abitibi rocks are komatiitic and the rocks of Pechenga tholeiitic. The experimental results of Rajamani and Naldrett (1978) suggest that the MgO content of the parental magma calculated for the rocks of Abitibi, Pechenga and Suomussalmi might be 8—12 wt.%.

In the ternary Fe—Cu—S and Fe—Ni—S diagrams, the average chemical compositions of different sulphide ore bodies (Table 9) in Suomussalmi plot near the Fe—S line (Fig. 15). The scattering of the points A···E at Peuraaho follows the magmatic layering of the ultramafic lens. Thus, the Ni content is highest in the topmost part of the lens (D ore body) and lowest at the bottom. The Hietaharju points are of roughly the same composition which probably indicates later re-equilibration.

In the ternary system Cu—Fe—S most of the points plot in the field of monoclinic pyrrhotite + pyrite + chalcopyrite solid solution + vapour at a temperature of 200°C (Kullerud *et al.* 1969). The composition of

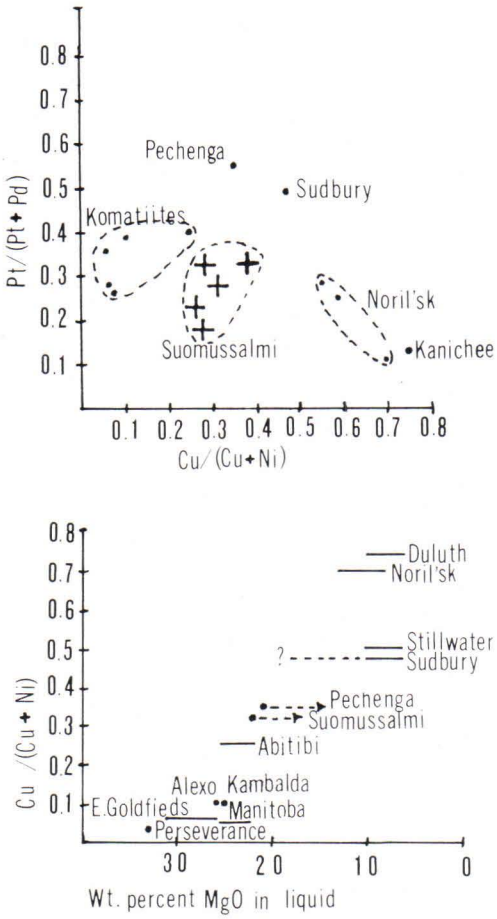

Fig. 14. Two diagrams drawn after Naldrett and Cabri (1976) illustrating the relations between Pt/(Pt + Pd) and Cu/(Cu + Ni) ratios and the composition of the host rock.

Table 9

Bulk compositions of sulphide phase in different ore bodies calculated from average analyses (Tables 6 and 8) using the compositions of different sulphide minerals. All figures are weight percentages.

Ore body	Fe	Cu	Ni	Co	S	As	Mode
Hietaharju A	57.08	2.27	3.59	0.26	36.37	0.43	cp 6.7 pn 10.3 po 82.1 grs 0.9
Hietaharju B	55.45	1.93	4.22	0.22	38.17	—	cp 5.7 pn 12.1 po 82.2
Hietaharju C	55.94	1.40	3.71	0.24	38.31	0.40	cp 4.1 pn 10.0 po 85.0 grs 0.9
Hietaharju D	55.16	1.80	4.53	0.23	38.28	—	cp 5.2 pn 13.0 po 81.8
Peura-aho A	52.99	2.44	6.35	0.37	37.85	—	cp 7.1 pn 18.3 po 74.6
Peura-aho B	45.68	0.94	2.25	0.09	51.04	—	cp 2.7 vl 2.6 po 8.4 py 86.3
Peura-aho D	49.74	3.42	9.21	0.79	36.84	—	cp 9.7 pn 25.8 po 64.5
Peura-aho E	57.72	0.66	2.06	0.23	39.32		cp 1.9 pn 6.0 po 92.1

cp = chalcopyrite; pn = pentlandite; po = pyrrhotite; grs = gersdorffite; vl = violarite; py = pyrite.

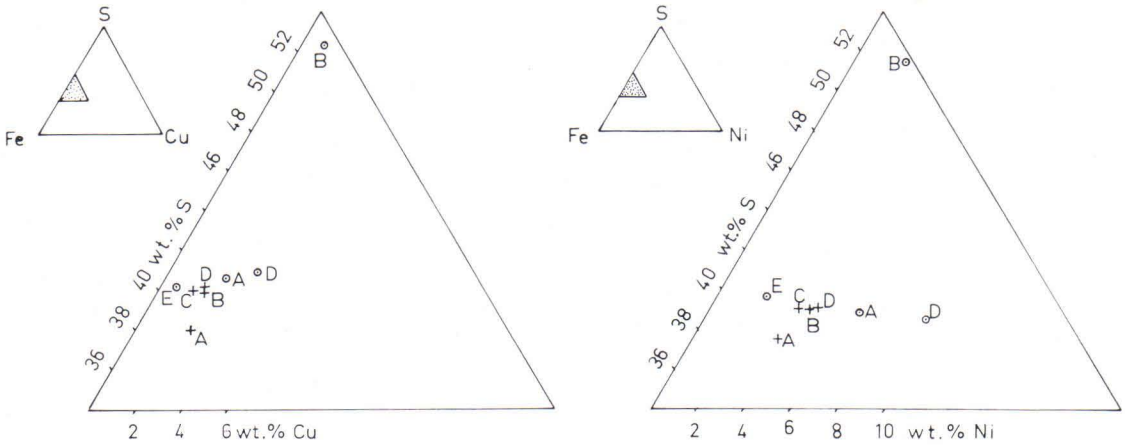

Fig. 15. Sulphide phase composition in ore lenses in the Hietaharju and Peura-aho deposits plotted in Cu-Fe-S and Fe-Ni-S ternary diagrams. Open circles = Peura-aho ore lenses; letters refer to different ore bodies; crosses = Hietaharju ore lenses.

Hietaharju A ore body plots in the field of chalcopyrite solid solution + hexagonal pyrrhotite + monoclinic pyrrhotite + vapour or in the field of chalcopyrite solid solution + cubanite solid solution + hexagonal pyrrhotite + vapour. The composition of the Peura-aho B ore body plots in the field of pyrite + monoclinic pyrrhotite + chalcopyrite solid solution + vapour, but near the pyrite corner indicating large sulphur content.

The ternary system Fe—Ni—S shows the same scattering in the points. Most of the points of Hietaharju plot in the field of hexagonal pyrrhotite + monoclinic pyrrhotite + pentlandite + vapour at 130°C. The Hietaharju A ore body plots in the field of hexagonal pyrrhotite + troilite + pentlandite + vapour at 130°C. The Hietaharju A ore body plots in the field of hexagonal pyrrhotite + troilite + pentlandite + vapour. The Peura-aho sulphide phase compositions plot in the field of pyrite + pentlandite + monoclinic pyrrhotite + vapour, the Peura-aho B ore body near the pyrite-corner (Kullerud *et al.* 1969). The exceptionally high sulphur content of the Peura-aho B ore body is best explained by sulphurisation.

ORE MINERALS

As in most Ni-Cu deposits the major ore minerals in the Suomussalmi deposits are pyrrhotite, pentlandite and chalcopyrite. Oxide ore minerals containing chromium, iron and titanium are fairly common. The calculated amount of magnetite varies from 6.9 to 67.8 wt.% of the ore minerals. In some samples arsenides are among the major minerals. The rare platinum-group minerals, gold and tellurides occur mostly in the low-temperature parageneses. Alteration products of iron-nickel sulphides are common.

Pyrrhotite

Pyrrhotite occurs in every ore-mineral assemblage of the Suomussalmi sulphide deposits. It has been shown experimentally that there are at least ten different structural modifications of pyrrhotite indicating different chemical compositions and temperatures of stability. The cell parameters of the pyrrhotite varieties are multiples of the basic NiAs structure. The high-temperature hexagonal form has a 1 C lattice, which is the original NiAs structure. The hexagonal high-temperature pyrrhotite melts at 1190°C. Below 308°C the hexagonal MC type ($3.0 \leq M \leq 4.0$) becomes stable. Monoclinic 4 C-type pyrrhotite is stable below 254°C. Troilite, the hexagonal 2C pyrrhotite is stable below 140°C (Rising 1973, Craig and Scott 1974, Kissin 1974, Power and Fine 1976).

The normal pyrrhotite is reddish brown, is strongly anisotropic and has a clear reflection pleochroism and a reflectivity of R = 34.5—40.7 % at a wave length of 546 nm (Ramdohr 1969, Henry 1977). Optical distinction between the hexagonal and monoclinic varieties is difficult, even impossible. Etch reagents have been used, but with questionable results, the etch reaction rates differing according to the orientation of the grains (Schneiderhöhn 1952, p. 190).

The pyrrhotite in the samples studied is usually granular. In some samples deformation has produced lamellar texture and flattening of the grains. Inclusions are numerous and common. The progressive crystallisation

Table 10

Composition of pyrrhotite in Suomussalmi samples analysed by XRD.

Location of samples	Number of samples	Average of $^{d}102$	Average of $^{d}408$	Weight % hex po	Fe content (at. %) in hex. po
PA [1]	8	—	2.058 (0.003)	0	—
PB [2]	6	2.060	2.057 (0.002)	0—20	46.79
PE	2	2.065 (0.004)	2.056 (0.001)	15—20	46.88—47.59
HA	4	2.070 (0.003)	—	60—100	47.41—47.96
HC	4	2.069 (0.005)	2.055	15—100	47.14—48.05

[1] First letter: P = Peura-aho; H = Hietaharju. Second letter = orebody.
[2] Hexagonal pyrrhotite was found in three samples.

Table 11

Chemical composition of pyrrhotite in the ore bodies of Suomussalmi. Analyst, J. Ottemann.

Sample locality	Weight % Fe	Ni	Co	Cu	S	Atomic % metals	Remarks
Peura-aho A	59.9	0.63	0.06	0.04	40.05	46.53	monoclinic
Peura-aho B	59.7	0.73	0.05	0.27	40.21	46.43	monoclinic
Hietaharju A	62.4	0.24	0.08	—	37.14	50.02	hexagonal
Hietaharju C	60.6	0.30	0.09	0.02	39.49	47.12	monoclinic

of the monosulphide solid solution (mss) has produced a large variety of inclusions: euhedral magnetite, cubanite, chalcopyrite, sphalerite, gersdorffite, pyrite, marcasite. Especially noteworthy are the pentlandite exsolution flames orientated along the basal plane of the pyrrhotite. In the Peura-aho A ore bodies pyrrhotite and other sulphides have been replaced by serpentine minerals, which has given rise to a very fine-grained dissemination. The intergrowths with other minerals are usually simple, and granular pyrrhotite forms a matrix with chalcopyrite in the massive ore samples. Pyrrhotite is often replaced by lamellar marcasite or an »intermediate product» in the weathered samples (Ramdohr 1969, pp. 592—598). »Bird's eye» texture is also common in the weathered samples.

The pyrrhotite was studied by XRD using the method of Arnold (1962, 1966) and Arnold and Reichen (1962). In this method the 2Θ-angle and the intensity of the 102 peak of hexagonal pyrrhotite and the intensity of the 408 and 408 peaks of monoclinic pyrrhotite are used to determine the metal content in hexagonal pyrrhotite and the proportional abundances of hexagonal and monoclinic modifications. Sixteen samples from Peura-aho and eight samples from Hietaharju were studied by this method using Mn-filtered Fe radiation and a scanning speed of $^{1}/_{2}°$ a minute. The results are given in Table 10. The measurements indicate that the pyrrhotite in

Peura-aho is mainly monoclinic. The hexagonal variety has been observed in the B and E ore bodies, especially in samples from deeper levels. At Hietaharju the pyrrhotite is mainly hexagonal.

The microprobe analyses (Table 11) demonstrate that the pyrrhotite in the Hietaharju A ore body is iron-rich, with 50.02 atomic % metals. In the Hietaharju C ore body the chemical composition corresponds to that of the monoclinic 4 C type with 47.12 atomic % metals. In the Peura-aho samples, the chemical composition lies in the stability field of monoclinic pyrrhotite + pyrite or monoclinic pyrrhotite + smythite (Power and Fine 1976). In the samples from the Hietaharju A orebody the composition is nearly that of the stoichiometric FeS, where Fe is diadocically replaced by very small amounts of Ni and Co. In the monoclinic samples the percentages of Ni and Cu are higher, as has been observed in other Finnish ore bodies (Papunen 1970, Kojonen 1974).

The lattice constants were calculated from the XRD peaks. For hexagonal pyrrhotite the average values are a 3.447 (0.005) Å and c 5.744 (0.010) Å calculated from the Hietaharju pyrrhotite (8 samples). For monoclinic pyrrhotite in the Peura-aho A orebody (6 samples, the lattice constants are a 11.906 (0.007) Å, b 6.874 (0.005) Å, c 22.783 (0.071) Å, and β_{max} 90°16′; in the Peura-aho B orebody (6 samples) a 11.909 (0.032) Å, b 6.867 (0.013) Å, c 22.830 (0.069) Å, and β_{max} 90°43′; in the Hietaharju C orebody (1 sample) a 11.906 Å, b 6.875 Å, c 22.660 Å, and β_{max} 90°14′. Several reflections overlap in the powder pattern of pyrrhotite which makes it difficult to measure the 2Θ values accurately. Therefore the calculated β angle of monoclinic pyrrhotite is usually too low. The calculated lattice constants, however, agree well with previously published values (Ramdohr 1975, p. 635, Power and Fine 1976, Vaughan and Craig 1978).

Mackinawite

Mackinawite was identified on the basis of its optical properties: strong reflection pleochroism from reddish brown to dark violet brown and intense anisotropism. The polishing hardness is slightly higher than that of chalcopyrite. Mackinawite was found as inclusions in pyrite together with chalcopyrite in the Peura-aho A orebody and as numerous inclusions in chalcopyrite in the Hietaharju C orebody. The chemical composition of mackinawite ranges from $(Fe, Ni, Co, Cu)_{0.993}S$ to $(Fe, Ni, Co, Cu)_{1.068}S$ (Schott *et al.* 1972). However, the general formula is usually written $Fe_{1+x}S$ (Takeno and Clark 1967, Craig and Scott 1974). The Ni content of mackinawite is often considerable, as reported by Vaughan (1969) from Transvaal, South Africa. The scanning electron microprobe pictures of the Hietaharju mackinawite (Fig. 16) also suggest that even here the mackinawite contains reasonable amount of nickel.

Pentlandite

Pentlandite is stable up to 610°C in the pure Fe—Ni—S system (Kullerud 1963). Natural and synthetic pentlandites containing Co have, however, a higher break-down temperature (Vaasjoki *et al.* 1974, Kojonen 1976). The pure Co pentlandite Co_9S_8 breaks down at 830°C (Kuznetsov *et al.* 1965). The common pentlandite »flames» are considered exsolution products of the monosulphide solid solution below 400°C (Naldrett *et al.* 1967).

In the Suomussalmi samples pentlandite occurs mainly as: 1) idiomorphic grains, 2) irregular interstitial bands between the pyrrhotite grains and 3) exsolution lamellae along the basal plane of pyrrhotite. The idiomorphic crystals are frequently octahedrons. The diameter of the grains varies from 0.5 mm in the Peura-aho A orebody to about 5 mm in

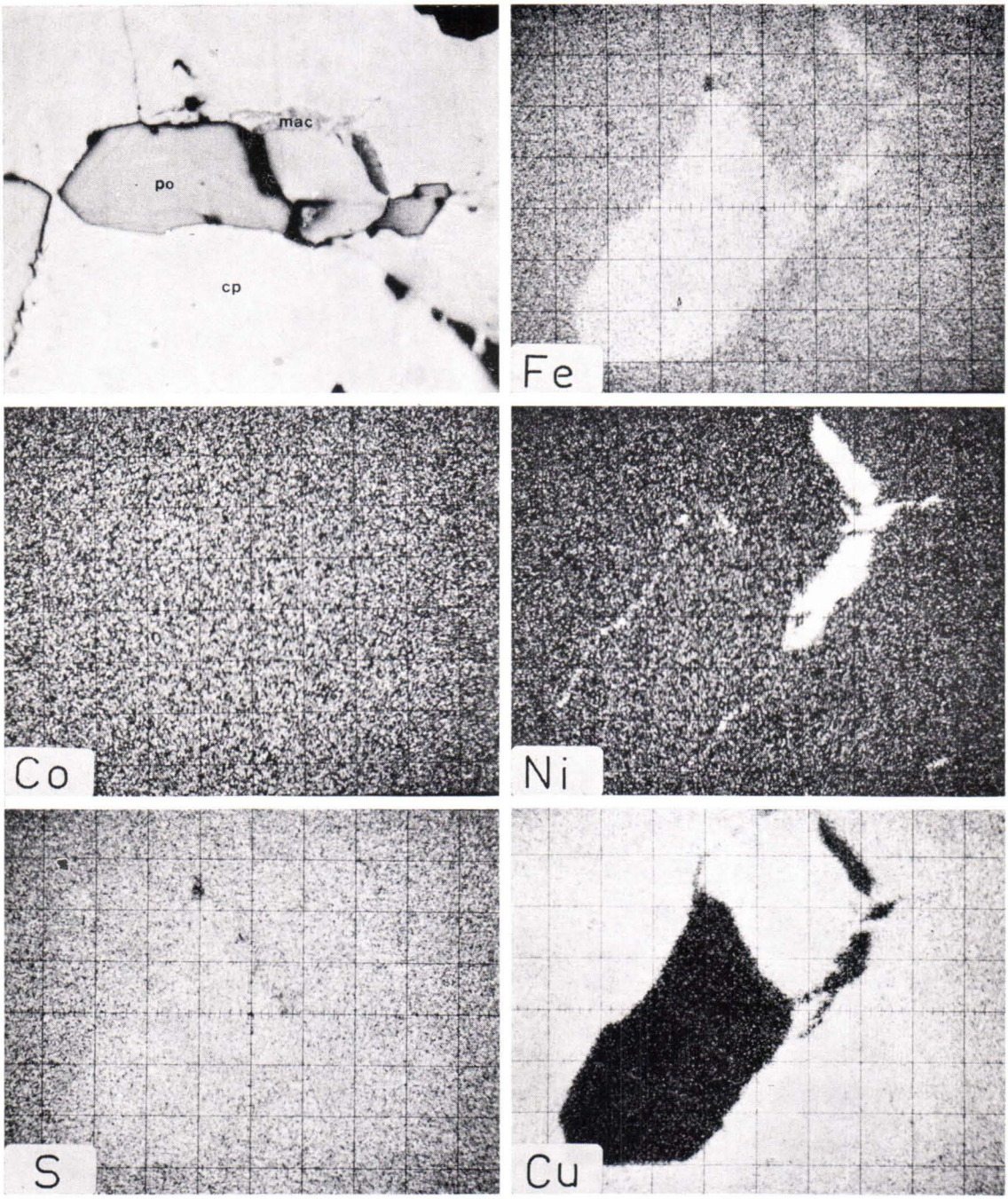

Fig. 16. Scanning electron microprobe pictures of mackinawite (mac) inclusions in chalcopyrite (cp). Sample Sms-20, 185.08 m, Hietaharju C ore body, 40 μm/#. Scanning pictures by J. Ottemann.

the Hietaharju A and C orebodies. The fractures are well developed owing to the large thermal expansion of pentlandite (Morimoto and Kullerud 1964). Inclusions of pyrrhotite in the form of a negative octahedron are not rare. Replacement by chalcopyrite along the fractures is common. Starting from the cleavage cracks, pentlandite has widely altered into violarite as a result of weathering. All phases from partly altered grains to violarite pseudomorphs after pentlandite are present.

The interstitial bands of pentlandite are free from inclusions. The separate grains in the bands are about 20 μm in size. In the Hietaharju samples the bands occur between chalcopyrite and pyrrhotite, whereas normally they exist between pyrrhotite grains. The lamellar exsolution »flames» are more yellowish in colour than the idiomorphic grains. The length of the lamellae is about 30 μm and the width is about 10 μm. Alteration into violarite was not observed in the lamellae.

The reflectance values of the Hietaharju pentlandite (Table 12) are higher than those of normal pentlandite but lower than those of cobaltoan pentlandite (Papunen 1970, Ramdohr 1975, p. 535, Henry 1977). The pentlandite grain assayed contained 2.22 wt.% Co (Table 13, 1). Papunen (1970) found a good correlation between reflectance and the Ni/Fe ratio in pentlandite. In his samples, however, the Co content of pentlandite was almost constant. From the data of Ramdohr (1975) it is evident that the increasing Co content enhances reflectance.

The Co content of the pentlandite decreases with progressive crystallisation: 2.22—1.44 wt.% in the coarse-grained pentlandite, 0.90 wt.% in the interstitial bands and very low in the »flame» pentlandite. The decreasing Co content in pentlandite has been reported previously in the Outokumpu-type ore deposits (Kouvo *et al.* 1959, Kojonen 1974).

The cell edge of cubic pentlandite decreases with increasing Co content (Knop *et al.* 1964, Kojonen 1976). The synthetic Co_9S_8 has a 9.932 Å (Kuznetsov *et al.* 1965), and pure $(Ni, Fe)_9S_8$ has a 10.066 Å. Thus, the measured a 10.052 (0.012) Å (Hietaharju A) and a 10.051 (0.015) Å (Peura-aho B) indicate a content of 0—20 mol % Co_9S_8 in the pentlandite.

The different pentlandite forms represent three different generations. The coarse-grained, often idiomorphic pentlandite crys-

Table 12

Reflectance and hardness (VHN) values of Suomussalmi pentlandite.

λ nm	1 R_{air}	2 R_{oil}	3 R_{air}
470	43.14	30.31	44.52
546	48.87	35.66	50.31
589	50.82	37.04	51.07
650	52.96	38.87	53.96

1 and 2: Sample H-1, Hietaharju A orebody; 3: Sample P-9, Peura-aho A orebody. Standard SiC, immersion oil Din 58884, Schott interference line filter, final polishing on Struers NAP cloth with 1 μm aluminium oxide.
VHN 225—243 p, mean 233 (load 100 p) of 15 measurements.

Table 13

Electron microprobe analyses of Suomussalmi pentlandites. Analyst, J. Ottemann.

	1	2	3
Fe wt. %	33.28	34.81	33.50
Ni	31.91	33.17	32.31
Co	2.22	1.44	0.90
Cu	0.06	0.04	0.05
S	32.19	31.63	34.24
Total wt. %	99.66	101.09	101.00
(Ni+Co)/Fe	1.03	0.99	0.99
Ni/Co	14.37:1	23.03:1	35.90:1

1. Coarse-grained pentlandite, Sms H-1, Hietaharju A orebody
2. Idiomorphic pentlandite, Sms-20, Hietaharju C orebody
3. Interstitial pentlandite, Sms-20, Hietaharju C orebody

Table 14

Chemical composition of chalcopyrite (1-4) and cubanite (6) in Suomussalmi samples. Analyst, J. Ottemann.

	1	2	3	4	5	6
Fe wt. %	31.10	31.07	30.00	30.74	30.43	41.32
Cu	33.77	33.47	34.02	34.20	34.63	22.06
Co	—	0.03	—	0.05	—	0.06
Ni	—	0.03	—	—	—	0.09
S	34.27	34.87	34.22	34.35	34.94	35.65
Total wt. %	99.14	99.47	98.24	99.34	100.00	99.18
Atomic Cu/Fe	0.954	0.948	1.000	0.978	1.000	0.469
Atomic Me/S	1.018	0.995	1.007	1.016	1.000	0.980

1. Hietaharju A, chalcopyrite
2. Hietaharju C, »
3. Peura-aho A, »
4. Peura-aho B, »
5. Calculated chalcopyrite $CuFeS_2$
6. Hietaharju C, cubanite

tallised at 610—650°C as exsolution product from the monosulphide solid solution (Kullerud 1963, Kojonen 1976). Next to crystallise were the interstitial rims of pentlandite, probably below 400°C (Naldrett *et al.* 1967). The pentlandite »flames» are the result of exsolution from Ni pyrrhotite below 300°C (Hawley 1962, p. 57, Naldrett and Kullerud 1967). The exsolution might have been associated with lattice deformation of the host pyrrhotite (Papunen 1970). Appropriate temperatures would be those of beta-transition at 308°C and of hexagonal-monoclinic transition at 254°C.

Chalcopyrite

In the system Cu—Fe—S, the tetragonal chalcopyrite becomes stable below 557°C. Above 557°C chalcopyrite decomposes into intermediate solid solution (iss) and pyrite (Craig and Scott 1974). On the basis of different quenching behaviour from 600°C Cabri (1973) has divided the iss field into three zones: zone 1 (S-rich portion) gives, in quenching, chalcopyrite + iss, zone 2 (S-deficient region) quenches to a phase exhibiting a primitive sphalerite-type cubic cell and zone 3 (central and Cu-rich part of the iss) quenches to the primitive cubic phase + chalcopyrite or mooihoekite.

The chalcopyrite in the Suomussalmi samples is often twinned and consists of lamellae of uniform thickness or of acicular »oleander leaf» lamellae (Ramdohr 1975, pp. 567—569). The twinning is caused either by deformation or by the transformation of high-temperature phases into normal tetragonal chalcopyrite. The twinned chalcopyrite grains are anhedral, and granular in shape. Chalcopyrite is associated with most of the ore minerals at Suomussalmi. Some of these can be interpreted as having crystallised before chalcopyrite (idiomorphic chromite and magnetite, pentlandite); some afterwards (cubanite, mackinawite, sphalerite). The order of crystallisation of some inclusions remains enigmatic (gersdorffite, altaite, pyrrhotite). Chalcopyrite has been replaced by serpentine in the serpentinite samples from the Peura-aho A orebody. Chalcopyrite replaces the

idiomorphic grains of pyrite and pentlandite along the cleavage fractures and, together with pyrrhotite, usually forms the matrix of sulphide-rich samples. The lattice parameters studied by XRD are a 5.28—5.29 Å and c 10.40—10.50 Å. The chemical composition (Table 14) shows minor fluctuations from the ideal $CuFeS_2$. In the Hietaharju A orebody the chalcopyrite is rich in metals but the Cu/Fe ratio less than 1 indicates an excess of Fe. In the Hietaharju C orebody chalcopyrite is slightly deficient in Cu. It is almost identical at Peura-aho except for the small excess of metals due to the Fe in the Peura-aho B orebody.

Cubanite

Small amounts of cubanite occur in the samples from the Hietaharju C orebody as irregular rims in chalcopyrite, between chalcopyrite and pyrrhotite and between pyrrhotite grains. Lamellar cubanite was not observed. Orthorhombic, naturally occurring cubanite is stable up to 200—210°C (Cabri *et al.* 1973). Chemical analysis (Table 14) gives a formula $Cu_{0.94}Fe_2S_3$. In the Cu—Fe—S system at 300°, the chemical composition plots in the iron-rich end of the iss in equilibrium with chalcopyrite + pyrrhotite + vapour. Two modes of origin are possible for cubanite: 1) cooling of the iron-rich iss and 2) reaction between chalcopyrite and pyrrhotite in cooling.

Pyrite

Pyrite is stable up to 743°C at which it breaks down to hexagonal 1 C pyrrhotite + sulphur (Kullerud and Yoder 1959). The pyrrhotite— pyrite solvus has been studied in detail by Arnold (1962), Toulmin and Barton (1964), Barton and Skinner (1967), Burgmann *et al.* (1968), Scott and Barnes (1971) and others. These findings indicate that the stability of pyrite depends on coexisting pyrrhotite composition, temperature, pressure and activities of FeS and sulphur. Below 300°C the situation is complicated by the appearance of pyrrhotite superstructures. In the presence of sulphur- and iron-bearing solutions, pyrrhotite reacts and changes to a more iron- or sulphur-rich modification, whereas pyrite remains unchanged in composition. As a result of simple oxidation pyrrhotite can become richer in sulphur and even change to pyrite or marcasite. At a temperature as low as 150°C in the presence of excess sulphur but not below 400°C in the absence of sulphur the marcasite can be inverted into pyrite (Kullerud 1967, Craig and Scott 1974). Marcasite coexisting with pyrite can be synthesised at up to 423°C in the presence of water but not in its absence.

Pyrite as a major sulphide mineral occurs only in the Peura-aho B orebody as euhedral to subhedral grains replaced by chalcopyrite along the cleavage cracks. Along the margins of the Peura-aho B ore lens pyrite often contains anisotropic, cryptocrystalline marcasite. Other inclusions are chalcopyrite, magnetite and chromite. In the Peura-aho A orebody pyrite is sometimes observed as euhedral grains with inclusions of chalcopyrite and mackinawite; in the sulphide veins it shows myrmekitic intergrowth with magnetite. Other weathering products are marcasite lamellae along the 0001 plane of pyrrhotite and zoned pyrite—marcasite »bird's eye» textures. Black schist samples often contain several modifications of pyrite and marcasite. The lattice parameters obtained for pyrite by XRD are: a 5.416 (0.005) Å (Peura-aho A), a 5.415 (0.003) Å (Peura-aho B) and a 5.416 (0.007) Å (Hietaharju). The microprobe analyses (Table 15) show that the pyrite in the Peura-aho A orebody has a high Co content and is metal deficient, whereas the pyrite in the Peura-aho B orebody is nickeliferous and sulphur deficient compared with the cal-

Table 15

Chemical composition of pyrite in Peura-aho. Analyst, J. Ottemann.

	1	2	3
Fe wt. %	45.55	45.34	46.55
Co	1.04	0.08	—
Ni	—	1.46	—
Cu	—	—	—
S	54.98	52.59	53.45
Total wt. %	101.57	99.47	100.00
Atomic Me/S	0.486	0.511	0.500

1. Peura-aho A
2. Peura-aho B
3. Calculated FeS_2

culated pyrite composition. This obviously reflects different kinds of pyrite crystallisation. The reflectance and hardness values measured for the Peura-aho A pyrite are: R(%) 50.0 (470 nm), 53.6 (546 nm), 53.9 (589 nm), 53.7 (650 nm) and VHN 1018–1097 f (100 p load). The reflectance values are higher than those given by Simpson *et al.*, in Henry (1977) for nickelian pyrite but slightly lower than the values for normal pyrite given by the same authors. The VHN values of pyrite in the Peura-aho A orebody resemble those of nickelian pyrite (Henry, op. cit., cards 1.7120.1—1.7120.3).

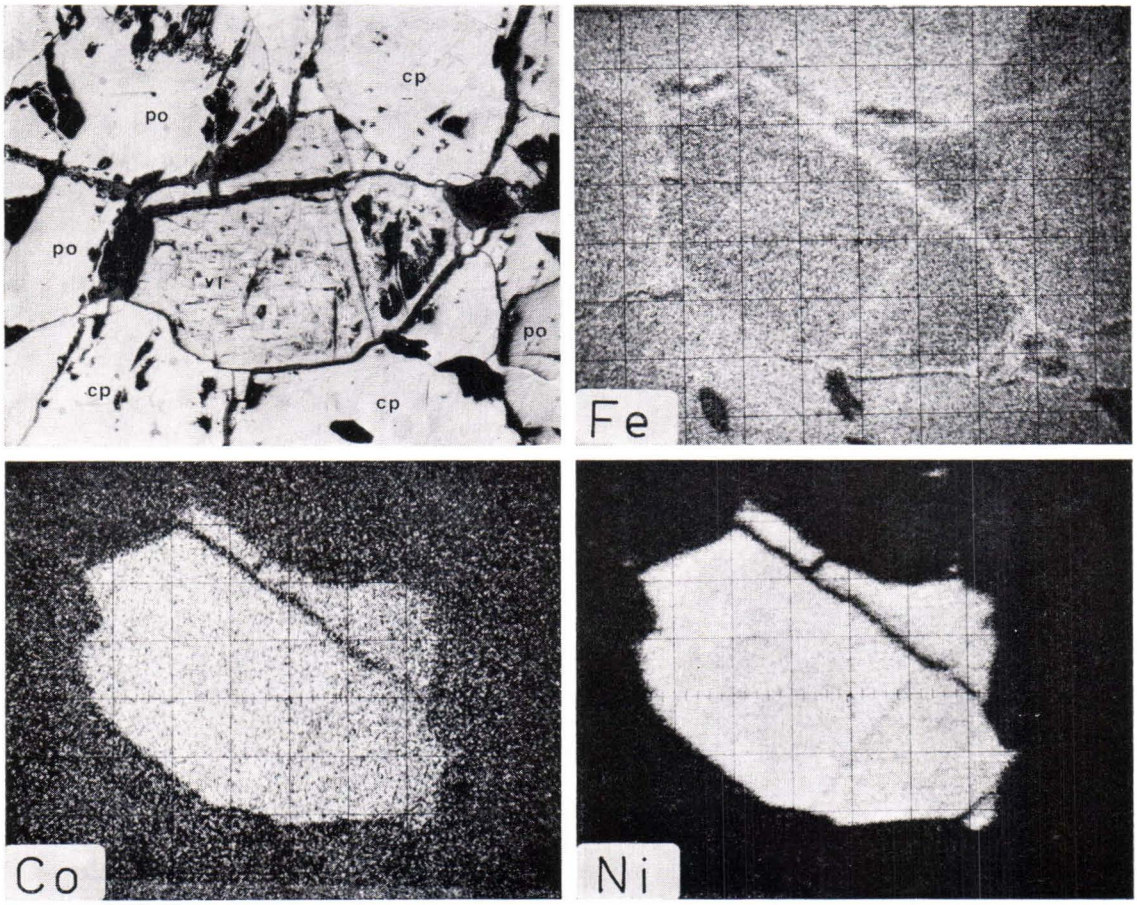

Fig. 17. Violarite (pentlandite-pseudomorph) in a matrix of pyrrhotite (po) and chalcopyrite (cp) Sample PB-52, Peura-aho B ore outcrop, 60 μm/#. Electron microprobe scanning pictures by J. Ottemann.

Violarite

Violarite is a common alteration product of pentlandite in the Peura-aho and Hietaharju sulphide ore samples. The alteration starts at the grain margins and cleavage cracks and often the whole grain of pentlandite has been replaced pseudomorphically by violarite. Violarite was formed at a very low temperature through weathering caused by meteoric waters (Craig and Scott 1974). Because of the heterogenity of violarite quantitative chemical analysis was not possible. Nevertheless, the electron microprobe scanning pictures (Fig. 17) show that violarite also contains some Co. The lattice parameter obtained by XRD a 9.46 (0.007) Å is nearly the same as reported by Craig (1971) for the $FeNi_2S_4$ end member in the violarite—polydymite sulphide—spinel series M_3S_4 (where M is Fe,Ni,Co,Cu,Cr).

Sphalerite

Sphalerite occurs in chalcopyrite as rare anhedral grains and sometimes between pyrrhotite grains. According to microprobe analysis it contains in wt. %, Zn 59.91, Fe 6.46, Cu 0.30, Ni 0.01 and S 33.63 totalling 100.31 with an atomic Me: S ratio of 0.989, (analyst J. Ottelman). Thus, the sphalerite in Peura-aho contains FeS 11.24 mole % giving a calculated a 5.415 Å (Barton and Toulmin 1966). The FeS content of sphalerite in Peura-aho correspond to the mineral pair monoclinic pyrrhotite—sphalerite in equilibrium below 250°C (Scott and Kissin 1973).

Arsenides

Gersdorffite—cobaltite was found in massive ore samples from the Hietaharju A and C orebodies. The crystals are usually cubic, euhedral or subhedral, and often corroded at the margins. Intense illumination by crossed nicols revealed zoning in the crystals, the core being isotropic and the rims anisotropic. Microprobe analyses (Table 16) show differences in chemical composition between the core and the rim of a given crystal: the core contains more Ni and As and less Fe, Co and S than the rim. A lattice constant of a 5.638 (0.004) Å was calculated from the XRD peaks. The average VHN is 749 (15 measurements, 100 p load) and R_{air} (589 nm) is 49.7 %. The chemical formula of the grain analysed from the Hietaharju A orebody is $(Ni,Fe,Co)_{1-x}$ AsS. The ratio As:S is more than 1 in the core and less than 1 in the rim. For the grain analysed from the Hietaharju C orebody the formula can be written $(Ni,Fe,Co)_{1+x}$AsS. The lattice constant, VHN and R values, chemical analyses and optical observations indicate that the core of the grains is gersdorffite that becomes richer in Co, anisotropic cobaltite towards the rims. According to Ramdohr (1975, p. 890—891), the (Ni,Co,Fe):(S,As,Sb) ratio might range from 1:2 to 2:3 in the gersdorffite. The content of As in gersdorffite often considerably exceeds that of S. Although the formula for gersdorffite is NiAsS, some published analyses show high contents of Fe and Co. According to Bayliss (1969), cobaltite and gersdorffite form a complete cubic solid solution, which, depending on the initial composition of the cubic solid solution, breaks down into distorted phases below 700—400°C. At Hietaharju, the gersdorffite with a cell edge of a 5.64 Å breaks down into gersdorffite and cobaltite at a temperature of 470—480°C.

Magnetite, chalcopyrite, pentlandite, pyrrhotite, gold, tellurobismuthite and wehrlite occur as inclusions in gersdorffite (Fig. 19, 1, 3, 4).

Tellurides

The inclusions in gersdorffite were analysed qualitatively on a microprobe; in-

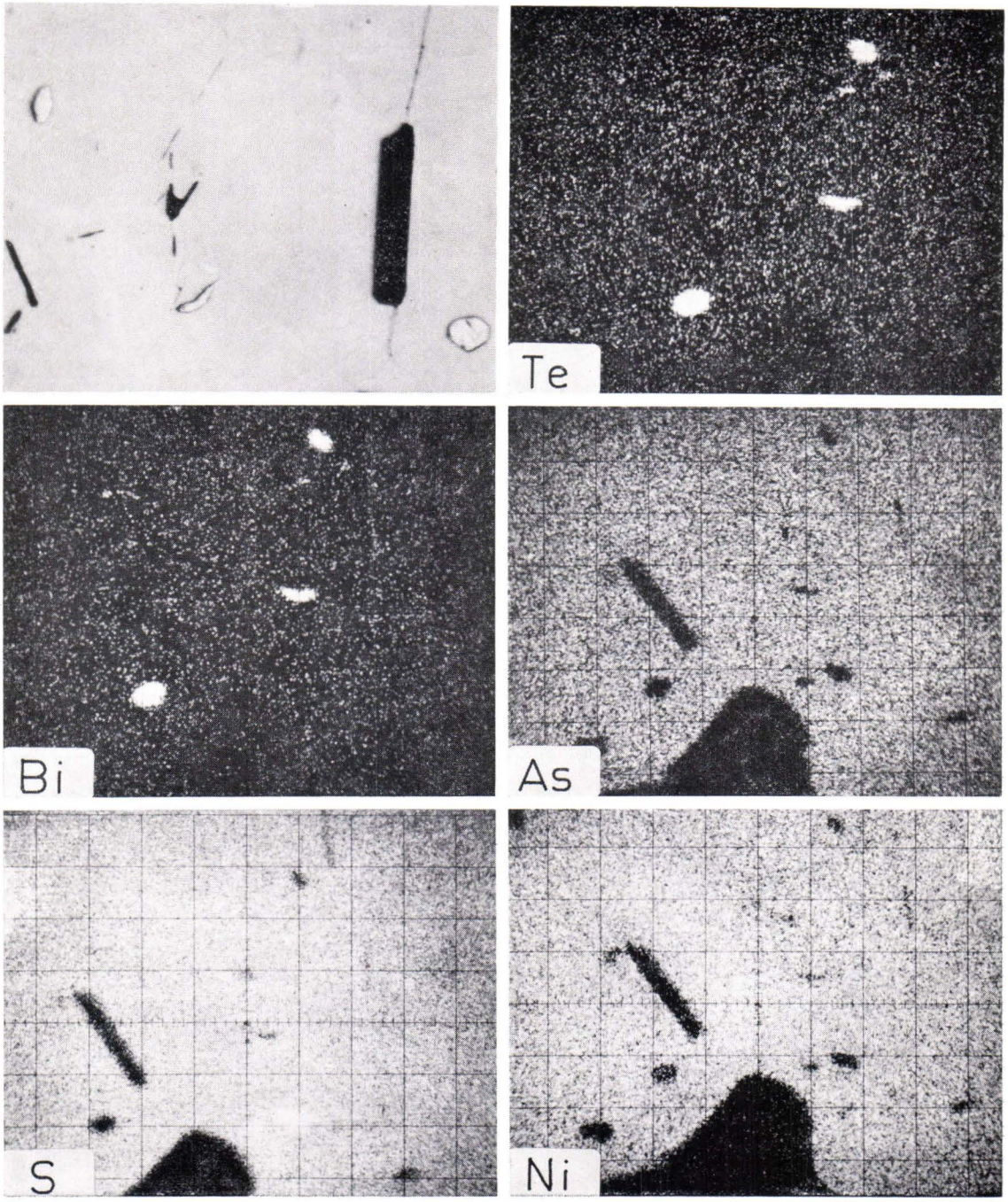

Fig. 18. Tellurobismuthite inclusions in gersdorffite. Optical picture at the upper left is the mirror image rotated by 180°. Sample Sms H-13, 178.15 m. Hietaharju C ore body, 30 μm/#. Electron microprobe scanning pictures by J. Ottemann.

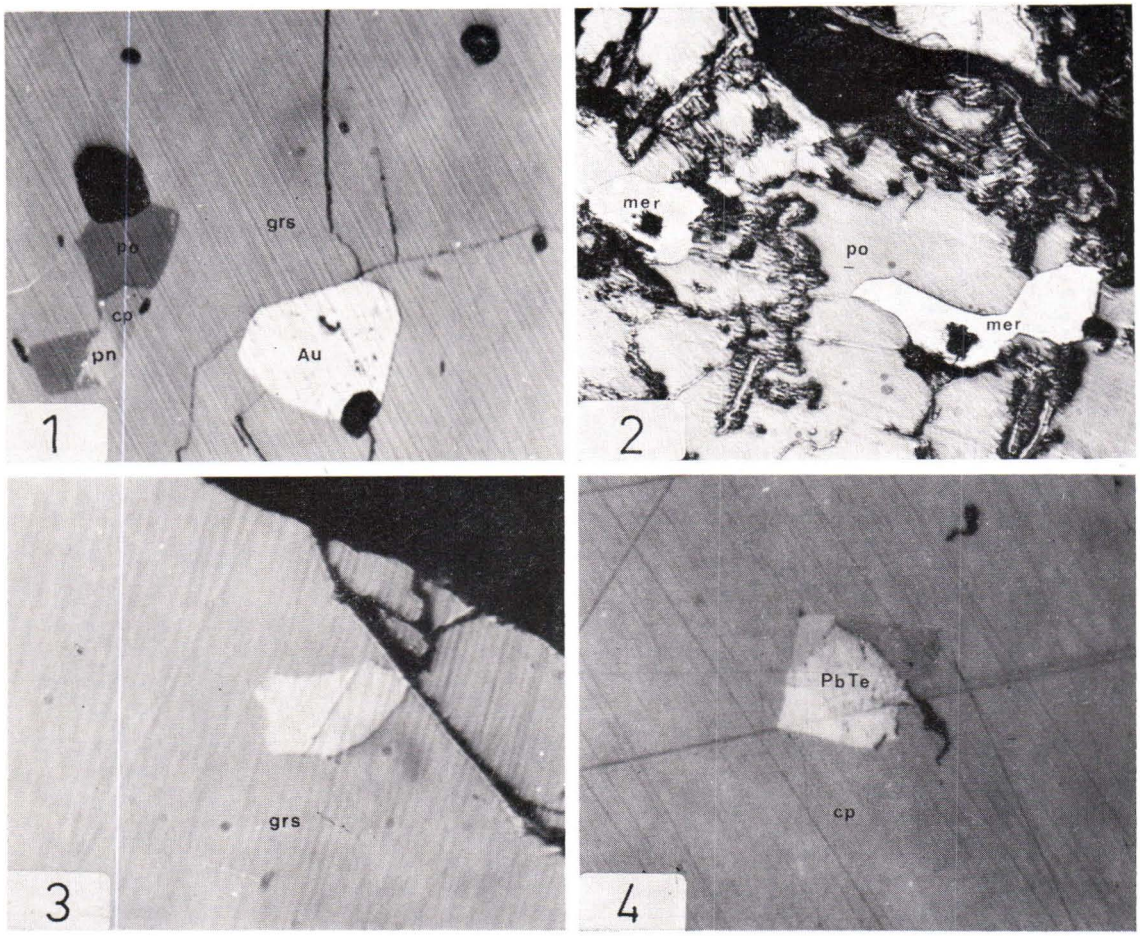

Fig. 19. 1. An euhedral inclusion of gold (97 wt.% Au, 4.1 wt.% Ag) in gersdorffite and an inclusion consisting of pyrrhotite (po), chalcopyrite (cp) and pentlandite (pn). Sample Sms H-1, 20.22 m, Hietaharju A ore body, N //, 520 x oil; 2. Merenskyite grains in a pyrrhotite matrix. Sample PB-72, Peura-aho B ore outcrop, N //, 140 x; 3. Wehrlite inclusion in gersdorffite (grs). Sample Sms H-1, 20.22 m, Hietaharju A ore body, N //, 900 x oil; 4. A heterogenous inclusion in chalcopyrite consisting of PbTe. Sample Sms H-7, 48.02 m, Hietaharju B ore body, N //, 1900 x oil.

dications of Bi and Te in a atomic ratio 1:1 and 2:3 were obtained (Fig. 18). These ratios are characteristic of tellurobismuthite and wehrlite.

An inclusion in the chalcopyrite of the Hietaharju A orebody (Fig. 19, 4) exhibited a qualitative composition of PbTe, altaite. The inclusion has, however, at least four different phases.

Merenskyite $(Pb,Pt)(Te,Bi)_2$ was found in the pyrrhotite matrix in the Peura-aho B orebody (Fig. 19, 2). Reflectance, hardness and semiquantitative chemical analysis of the grains are given in Table 17. The grains are anhedral and clearly anisotropic. The reflectance and chemical composition resemble closely that of the merenskyite reported by Kingston (1966) from Rustenburg mine. The

Table 16

Chemical composition of gersdorffite-cobaltite. Analysts, M. Rannela (1 a, b) and J. Ottemann (2).

	1		2
	a	b	
Ni wt. %	21.72	19.05	21.78
Fe	7.77	9.86	9.12
Co	5.27	6.27	7.55
As	46.07	43.50	46.23
S	19.02	20.57	14.64
Total wt. %	99.85	99.25	99.32
Atomic As:S	1.04	0.91	1.35
Atomic $\frac{Me}{(As+S)}$	0.495	0.496	0.616

1. Hietaharju A, sample Sms H-13, 178.15. a = core; b = rim. Calculated formulas:
   (a) $(Ni_{0.62}Fe_{0.23}Co_{0.15})_{0.99}(As_{0.51}S_{0.49})_2$
   (b) $(Ni_{0.54}Fe_{0.29}Co_{0.17})_{0.99}(As_{0.48}S_{0.52})_2$
2. Hietaharju C, sample Sms-20, 185.08. Calculated formula $(Ni_{0.56}Fe_{0.25}Co_{0.19})_{1.23}(As_{0.57}S_{0.43})_2$

Table 17

Reflectance, hardness and chemical composition (analyst, E. Hänninen) of merenskyite, Peura-aho B orebody, Suomussalmi.

λ nm	^{R}air %	^{R}oil %
470	60.9—64.6	50.2—54.9
546	64.2—66.4	54.2—57.2
589	64.7—67.0	55.9—59.6
650	66.6—68.6	56.3—58.9

Standards: WC 314 (air) and SiC (oil Din 58884)
Polishing: 1 μm aluminium oxide on Struers NAP cloth
Monochromator: Schott interference line filter
VHN: 55-81 sf Load: 25 p

Pd wt. %	26.2
Ni	1.0
Bi	6.24
Te	56.83
Total wt. %	90.27

Suomussalmi merenskyite, however, contains about 1 % Ni, which is absent at Rustenburg.

The phase relations in the system Pd-Bi-Te have been studied by Hoffman and MacLean (1976). Tellurobismuthite has a melting point of 585°C and wehrlite of 540°C. Stoichiometric merenskyite melts congruently at 740 ± 3°C. The melting point decreases with the substitution of Bi for Te. Thus, the merenskyite at Suomussalmi is stable below 720°C.

The Te-Bi minerals at Suomussalmi are associated with the host mineral gersdorffite—cobaltite and with native gold that occurs as inclusions in gersdorffite. Thus, the arsenides seem to have acted as collectors of Bi, Te, Au and Ag that, at lower temperatures, formed discrete phases, possibly in connection with the order-disorder transformation of the host gersdorffite. The occurrence of altaite in chalcopyrite shows that Te became enriched at later stages of crystallization. Although stable up to 720°C, merenskyite is a late mineral formed through a reaction between Pd liberated in latemagmatic and post-magmatic processes and Te and Bi which concentrated during later stages of crystallisation (Kingston 1966, Stumpfl and Tarkian 1976).

Ilmenite—hematite

Ilmenite occurs in the Suomussalmi samples mostly as discrete oblong grains that obviously crystallised after chromite—magnetite. Exsolution textures between magnetite and ilmenite are rare. Ilmenite is commonly altered into leucoxene. The analysed ilmenite turned out to be manganoan in composition with TiO_2 50.72, MnO 3.89 and FeO 46.29 wt. % totalling 100.90 wt. % (analyst K. Hämäläinen) corresponding to 8.99 mol. % pyrophanite in solid solution with ilmenite. If stoichiometry is assumed, 3.57 wt. % Fe remains to form hematite.

At temperatures above 600°C, Fe_2O_3 and $FeTiO_3$ are isomorphous and completely mis-

cible in all proportions. When the temperature drops below the solvus, two phases are separated. If the rock is cooled rapidly, however, the ilmenites remain unexolved. This is the case in many extrusive rocks that have been rapidly transported to the surface from considerable depth and quenched (Ramdohr 1975, p. 1943—1046).

Pure hematite phase is rare in the Suomussalmi samples. Hematite inclusions in pyrrhotite and chalcopyrite were found in some samples from the Peura-aho A orebody. The weathered samples from the Peura-aho B orebody contain an alteration product consisting of cryptocrystalline quartz and hematite.

Chromite—magnetite

The mode of occurrence and the chemical composition of the spinel phases reflect the changes in physical and chemical conditions during the cooling of the host silicate—sulphide melt and those caused by later serpentinisation (Evans and Frost 1975, Haggerty 1976, Groves *et al.* 1977) and metamorphism.

The Suomussalmi ore lenses and host rocks contain several spinel phases, which clearly crystallized in different circumstances.

First, euhedral-subhedral chromite grains are found in disseminated ore of the serpentine host rock. The grains are zoned, the rim being iron-rich and the core often cataclastic and replaced by magnetite along the fractures (Fig. 20). The light-coloured magnetite has reacted with the core and sometimes no more than a relic of the core is visible. The sulphide ore lenses also contain chromite grains, but these are not so clearly zoned as those in a silicate environment. Microprobe analyses (Table 18) demonstrate that the chromite in a silicate environment has higher Al and Mg contents than those enclosed in sulphides. Thus, it seems that the environment has controlled the composition of chromite during crystallisation. The Zn and Mn contents of the analysed chromites are high in all samples (Table 18, Fig. 22), but the highest values seem to be in the chromites enclosed in massive sulphides (Fig. 21). This observation confirms the suggestion of Groves *et al.* (1977) that high Zn contents in chromite indicate mineralised ultramafic sequences. Papunen *et al.* (1979) have also reported high Zn contents in chromite in mineralised ultramafic rocks in Finnish Lapland. The chromite has crystallised from silicate and sulphide magmas as the very first phase. The work of El Goresy and Kullerud (1969) shows that above 700°C there is a complete solid solution between $Fe_{1-x}S$ and $Cr_{1-x}S$. Thus it appears that Cr can easily enter into a sulphide melt. At a low oxygen fugacity, magnetite is unstable, but Cr may combine with small amounts of oxygen to form a Cr-rich spinel. At a slight increase in f_{O_2}, magnetite starts to crystallise (Irvine 1965, Czamanske *et al.* 1976, Haggerty 1976).

Second, the chromian magnetite rims around the chromite cores may have formed in a number of ways: 1) from Fe_3O_4 and $FeCr_2O_4$ that are completely miscible above 900°C or 2) by a reaction between chromite and the magnetite formed in the serpentinisation of ultramafic rocks of low metamorphic grade (Cremer 1969, Evans and Frost 1975, Ramdohr 1975, pp. 1002—1008, Groves *et al.* 1977).

Third, there is euhedral, slightly chromian or pure magnetite in the massive sulphide samples of the Peura-aho B and the Hietaharju A and C orebodies (Fig. 21). This magnetite contains often sulphide drop inclusions, which were apparently liquid at the time the host magnetite crystallised. Naldrett (1969) has shown that the spinels are stable together with pyrrhotite solid solution + liquid above 934°C. Depending on the Fe

Table 18

Electron microprobe analyses in wt. % of chromites and magnetites of Suomussalmi ores. The Fe^{2+} and Fe^{3+} were calculated from Fe_{total} assuming stoichiometry and using formulae $(Fe^{3+} + Al^{3+} + Cr^{3+} + V^{3+}) = 2$ $[(Fe_{total} - Fe^{3+}) + Mg + Mn + Zn + Ni]$ after subtracting Ti and an equivalent amount of R^{2+} to form ulvospinel. Parameter mg $= 100 \cdot Mg/(Mg + Fe^{2+} + Mn + Zn + Ni)$. Analysts, Dr. J. Ottemann, samples 6a, 6b; Kirsti Hämäläinen, samples 1-5, 7-10.

	1	2a	2b	3	4	5a	5b	6a	6b	7	8a	8b	8c	9	10a	10b
TiO_2	0.80	1.07	0.86	0.25	0.08	0.81	0.47	0.78	0.05	0.15	0.58	0.49	0.16	0.53	2.35	1.21
V_2O_3	0.40	0.30	0.30	0.37	0.37	1.09	1.09	—	0.14	0.13	0.21	0.14	0.14	0.21	0.68	0.37
Al_2O_3	7.52	1.45	—	—	—	2.49	0.94	10.74	0.31	0.42	10.73	0.14	—	—	13.30	2.59
Cr_2O_3	50.68	31.89	14.29	14.89	2.03	39.21	21.44	46.26	12.37	0.01	47.44	31.69	17.78	21.67	37.16	35.41
Fe_2O_3	11.86	35.53	54.57	53.35	68.15	27.61	47.54	13.61	55.26	68.76	12.16	37.41	52.11	48.04	18.37	30.93
FeO	27.56	30.12	30.20	30.34	31.69	24.02	26.28	25.83	29.36	31.12	26.35	28.74	29.24	30.48	27.57	29.21
MgO	0.25	—	0.79	—	—	—	—	1.36	0.30	—	0.73	—	—	—	0.53	0.20
MnO	0.90	0.56	0.56	0.08	0.08	4.37	4.36	1.76	0.50	0.04	1.35	1.67	1.67	0.80	1.28	1.15
NiO	—	—	—	—	—	—	—	—	0.01	0.09	0.05	0.03	0.03	—	0.04	0.04
ZnO	2.23	0.74	0.25	0.47	—	3.06	1.23	2.03	0.33	—	2.16	0.80	0.50	0.36	1.84	0.86
Total	102.20	101.66	101.83	99.75	102.40	102.66	103.35	102.37	98.63	100.72	101.81	101.11	101.63	102.09	103.12	101.97
Mol. %																
RCr_2O_4	69.23	46.96	21.56	22.66	3.03	56.65	31.46	61.47	18.89	0.02	63.15	46.91	26.37	32.13	49.87	51.51
RAl_2O_4	15.34	3.19	0.00	0.00	0.00	5.37	2.06	21.31	0.71	0.95	21.42	0.31	0.00	0.00	26.65	5.62
RFe_2O_4	15.43	49.84	78.44	77.34	96.97	38.00	66.48	17.23	80.40	99.04	1.85	52.78	73.63	67.87	23.49	42.87
mg	0.63	0	1.94	0	0	0	0	3.43	1.32	0	1.85	0	0	0	1.32	0.49

1. Sample Sms-25, 98.27 m. Hietaharju A, sulphide ore
2a. Sample Sms-28, 149.01 m. Hietaharju C, sulphide ore, dark coloured part
2b. Sample Sms-28, 149.01 m. Hietaharju C, sulphide ore, light coloured part
3. Sample PB-83, ore outcrop. Peura-aho B, sulphide ore } two different
4. Sample PB-83, ore outcrop. Peura-aho B, sulphide ore } grains
5a. Sample Sms-47, 106.73 m. Peura-aho B, sulphide ore } a zoined
5b. Sample Sms-47, 106.73 m. Peura-aho B, sulphide ore } grain
6a. Sample Sms P-7, 38.90 m. Peura-aho A, disseminated ore (core)
6b. Sample Sms P-7, 38.90 m. Peura-aho A, disseminated ore (rim)
7. Sample Sms P-9, 44.30 m. Peura-aho A, sulphide vein
8a. Sample Sms P-9, 44.30 m. Peura-aho A, disseminated ore (core)
3b. Sample Sms P-9, 44.30 m. Peura-aho A, disseminated ore (rim)
8c. Sample Sms P-9. 44.30 m. Peura-aho A, disseminated ore (separate rim)
9. Sample Sms P-13, 99.15 m. Peura-aho A, sulphide breccia
10a. Sample Sms P-14. 140.74 m. Peura-aho A, sulphide breccia (core)
10b. Sample Sms P-14. 140.74 m Peura-aho A, sulphide breccia (rim)

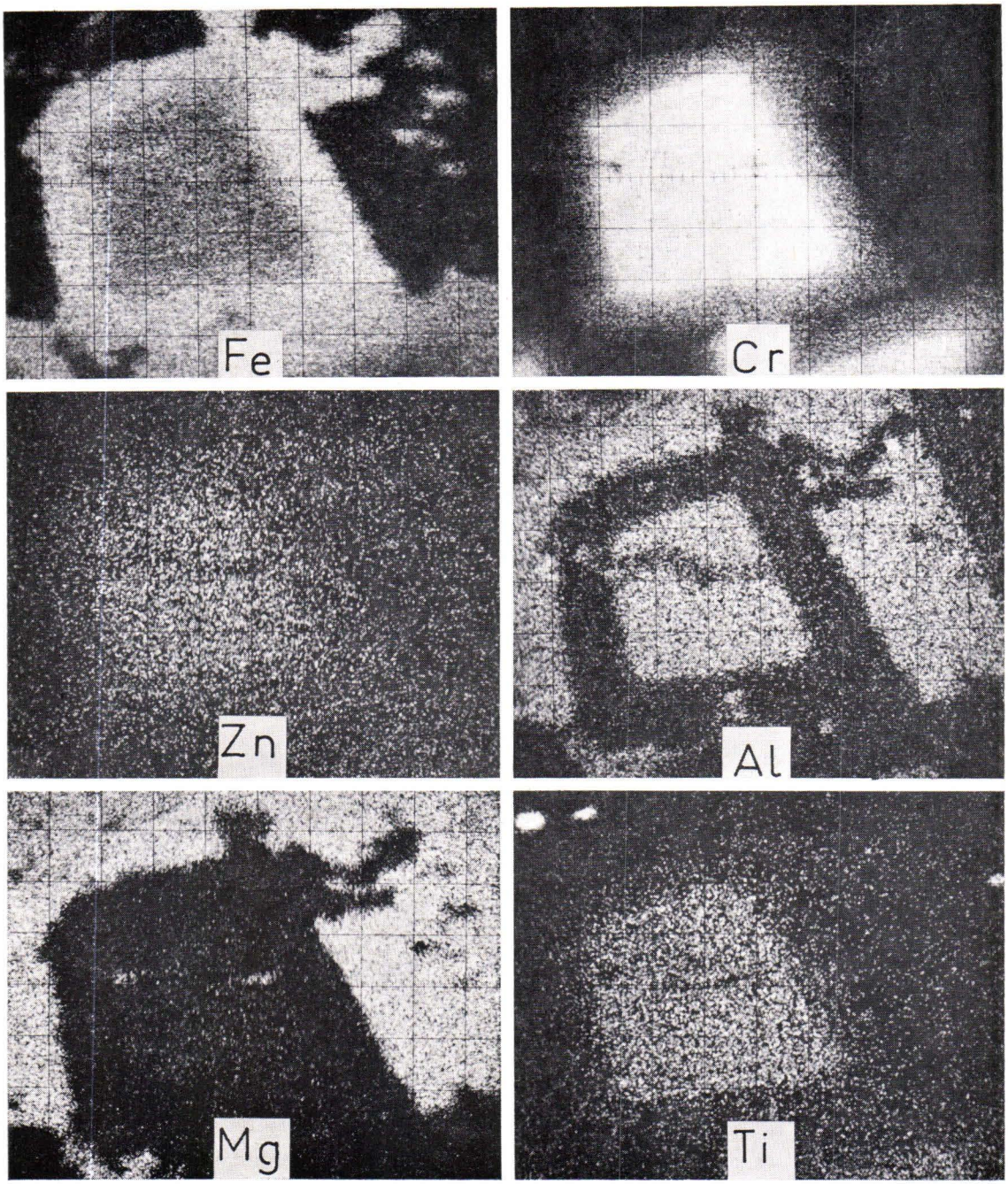

Fig. 20. Scanning electron microprobe pictures of zoned cataclastic chromite with a chromian magnetite rim. Sample Sms P-7, 38.90 m, Peura-aho A ore body, 34 μm/#. Analyst, J. Ottemann, compare analyses 6, 6a, table 18.

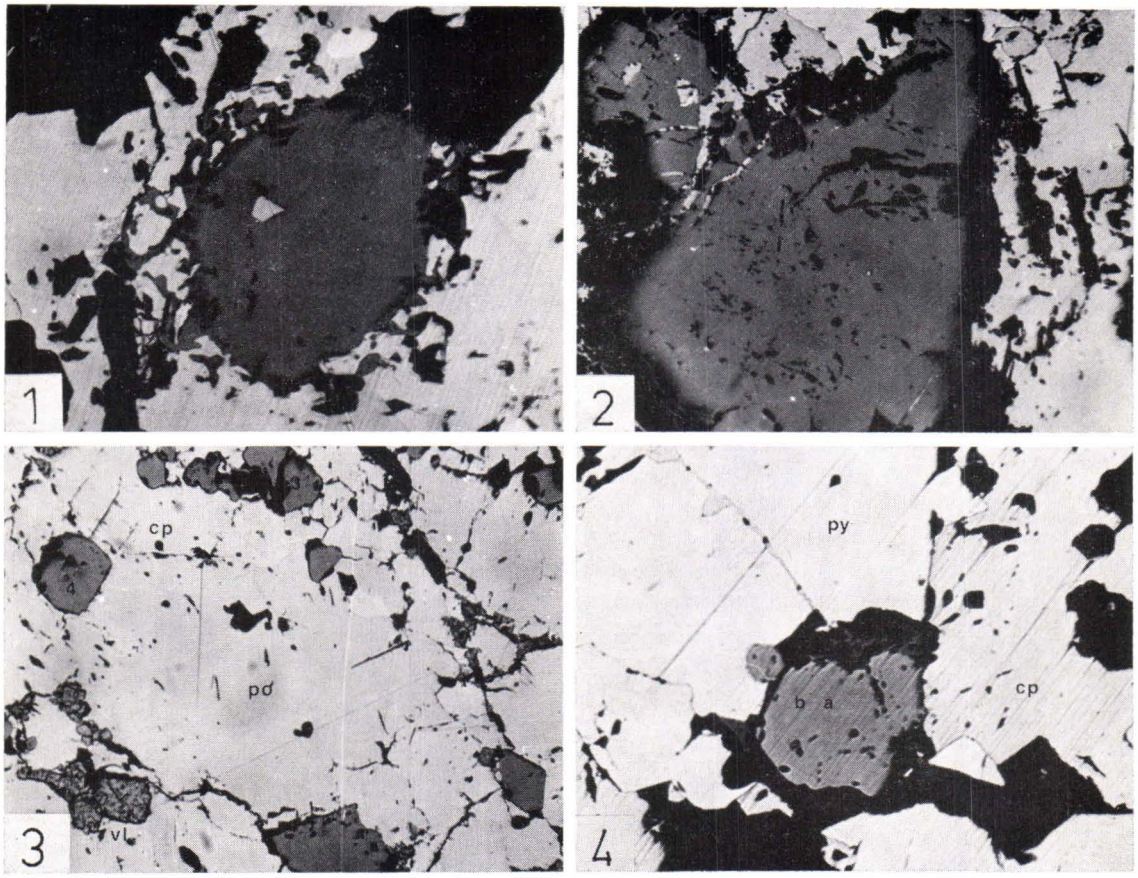

Fig. 21. 1. Slightly zoned chromite in sulphide ore (analysis number 1 in Table 18). Sample Sms-25, 98.25 m, Hietaharju A ore body, N //, 135 x; 2. Zoned chromite in sulphide ore (analyses 2a, b, Table 18). Sample Sms-28, 149.01 m, Hietaharju C ore body, N //, 35 x; 3. Homogeneous spinel grains (analyses 3 and 4, Table 18) in pyrrhotite(po)–chalcopyrite(cp)–violarite(vl) matrix. Sample PB-83, Peura-aho B ore outcrop, N //, 35 x; 4. Slightly zoned ferrochromite enclosed in pyrite(py)–chalcopyrite (cp) ore (analyses 5a, b, Table 18). Sample Sms-47, 106.73 m, Peura-aho B ore body, N //, 135 x.

content, the solidus temperature of the sulphide ore varies from 1020° to 1050°C. For the average composition of the ore bodies the solidus temperature in Peura-aho would be 1050°, and in Hietaharju 1030°C. Above these temperatures spinel, pyrrhotite solid solution and liquid are stable.

Fourth, in serpentinites of Peura-aho most of the spinel grains consist of ragged fine-grained magnetite disseminated throughout the serpentinite. This magnetite formed from the iron liberated from silicate minerals during serpentinisation (Groves *et al.* 1977).

Fifth, the sulphide-carbonate veins of serpentinite contain anhedral magnetite that is often cataclastic and replaced by serpentinite minerals. It crystallised together with the monosulphide solid solution before serpentinisation. Its chemical composition corresponds to that of pure magnetite (Table 18, anal. 7).

Sixth, in some weathered samples, pyrrho-

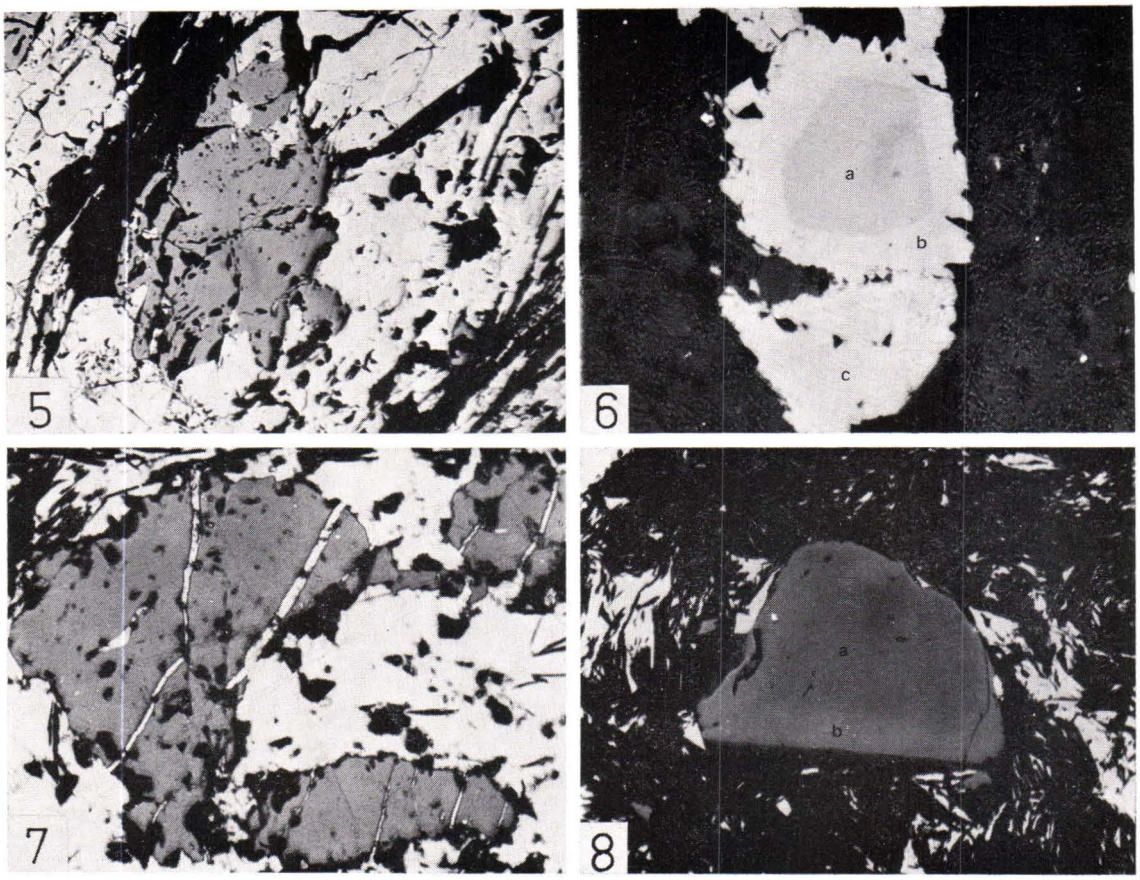

Fig. 21, continued. 5. Anhedral magnetite in a sulphide vein (anal. 7, Table 19). Sample Sms P-9, 44.30 m, Peura-aho A ore body, N //, 35 x; 6. Zoned chromite in serpentinite (analyses 8a, b, c, Table 18). Sample Sms P-9, 44.30 m, Peura-aho A ore body, N //, 135 x; 7. Ferrochromite replaced by pyrrhotite in sulphide breccia (analysis 9, Table 18). Sample Sms P-13, 99.15 m, Peura-aho A ore body, N //, 135 x; 8. Slightly zoned chromite in sulphide breccia (analyses 10a, b, Table 18). Sample Sms P-14, 140.74 m, Peura-aho A ore body N //, 135 x.

tite has altered into myrmekitic pyrite + magnetite. These are obviously replacement products formed at low pressure and temperature (Kullerud 1968).

To compare the chromites of Suomussalmi with those from Western Australia the chemical analyses of chromites and chromian magnetites are plotted in the composition triangle drawn after Groves *et al.* (1977) (Fig. 22). The diagram reveals that the chromites of Suomussalmi are much more ferrous than the Australian ones. Some of the Suomussalmi samples plot in the field of metasomatic, barren or weakly mineralized units. Three of these (numbers 6, 8 and 10) were taken from weakly mineralised serpentinites. As a whole, the ferrochromite—magnetite trend of Suomussalmi spinels resembles closely that of subaerially extruded tholeiitic suites characterised by spinels in Hawaiian lavas (Haggerty 1976).

The lattice constants of the spinels were

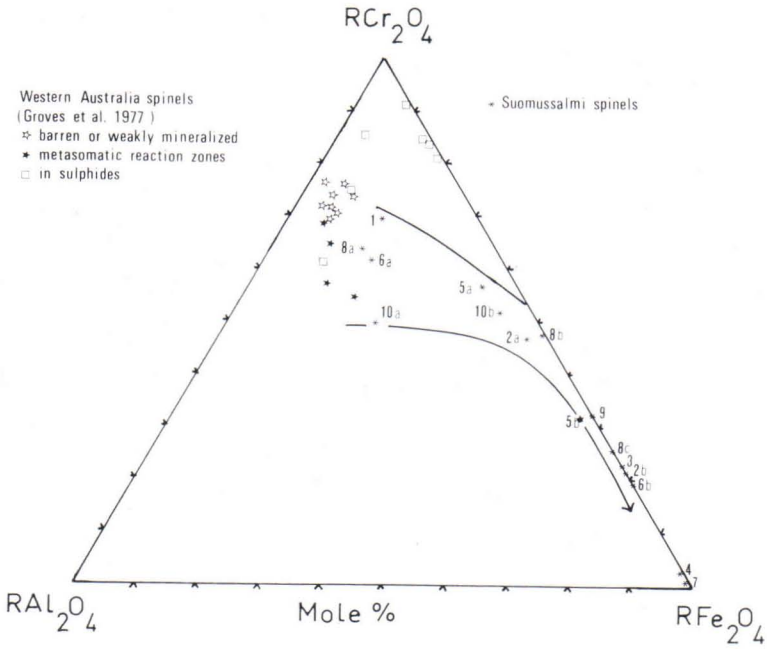

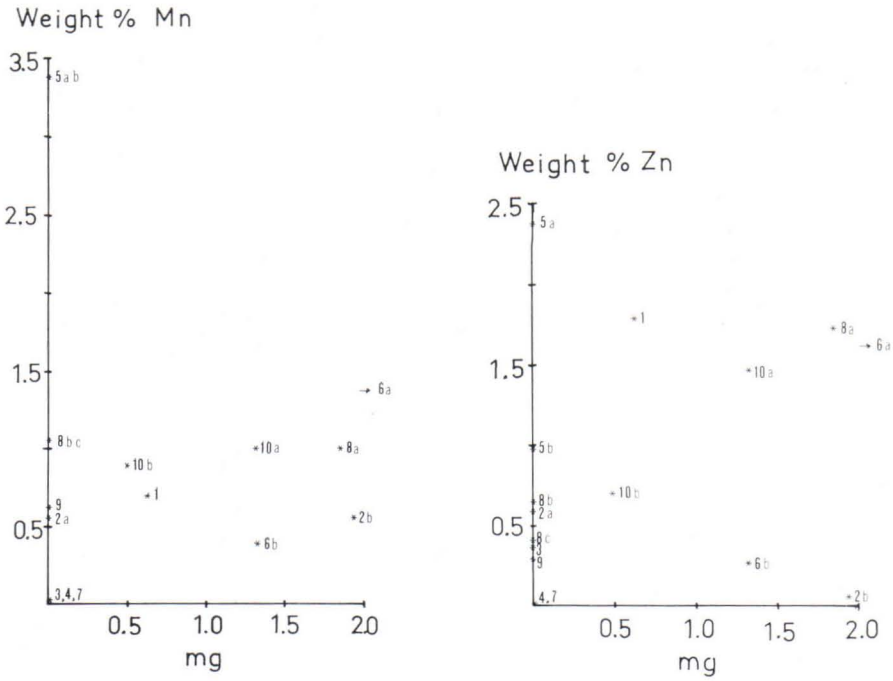

Fig. 22. The analysed spinels plotted in RCr_2O_4-RAl_2O_4-RFe_2O_4 composition triangle and Mn, Zn vs. mg diagrams. The numbers refer to analyses in Table 18.

calculated from diffractograms: a 8.40 (0.01) Å for magnetite in Peura-aho and Hietaharju, a 8.344 (0.006) Å for zincian chromite in Peura-aho. The corresponding values in literature are: a 8.396 Å for magnetite, a 8.345 (0.097) Å for zincian chromite and a 8.349 (0.003) Å for ferrochromite (Deer *et al.* 1962, Thayer *et al.* 1964, Cremer 1969 and Lindsley 1976).

Reflectance and hardness were measured in the core of zincian ferrochromite (Table 19). Owing to higher Fe and Zn contents the reflectance is distinctly higher than that in normal chromite.

Table 19

Reflectance (R_{air}) and hardness (VHN) values of chromites.

	1	2
λ nm	R %	R %
400	21.7	13.5
420	16.5	13.3
440	16.4	13.1
460	16.4	12.9
480	16.0	12.7
500	15.7	12.6
520	15.5	12.4
540	15.3	12.3
560	15.3	12.2
580	15.3	12.1
600	15.1	12.0
620	14.7	12.0
640	14.7	11.9
660	14.6	11.9
680	14.3	11.9
700	14.0	11.9
VHN	1192 ± 117 sf	1332 p
Load	100 p	100 p
Monochromator	Schott interference line filter	Zeiss glass prism
Final polishing	1 μm aluminium oxide on Struers NAP cloth	1 μm diamond on pellon
Standard	SiC	SiC

1. Peura-aho A orebody, core of a zoned chromite
2. Chromite, Bou Azzer, Morocco (Simpson *et al.* 1977)

SUMMARY AND CONCLUSIONS

The Suomussalmi nickel-copper deposits are located in a complex of serpentinites, talc—carbonate rocks, mafic volcanites, black schists, felsic schists and porphyries. Diamond drilling data, geochemical analyses and petrographic evidence suggest that the ultramafic rocks were deposited on the felsic schists and porphyries as cumulates of basaltic lavas. Accordingly, two cycles of volcanism can be distinguished in the Suomussalmi area (Fig. 23): I, early basaltic cycle terminating with rhyolitic volcanism and II, later basaltic cycle(s) with ultramafic cumulates, black schist, phyllite and mica schist interlayers with felsic volcanites, quartzites and conglomerates on the top. Both cycles are intruded by granites of different ages and by diabases.

In Kanowna—Kalgoorlie—Kurrawang area, Western Australia, the stratigraphic succession is very similar to Suomussalmi stratigraphy (Gee 1975); the lowermost sequence is a mafic association (Morelands Formation) overlain by felsic volcanic complex (Gindalbie Formation), which is unconformably overlain by a mafic sequence characterized by abundant rocks of the high-magnesium suite (Mulgabbi Formation). This is overlain by volcanic sedimentary rocks (Black Flag Beds), which is overlain by another mafic volcanic

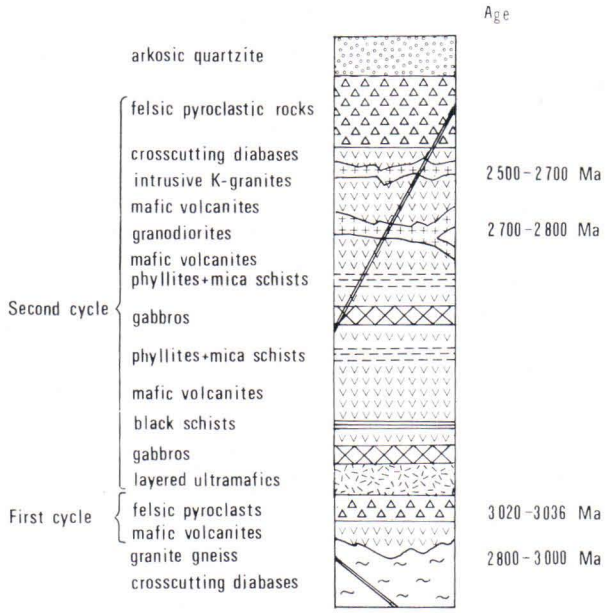

Fig. 23. Schematic stratigraphic section of the Suomussalmi area.

belt (Abbatoir Line) and felsic agglomeratic unit. The whole sequence is finally overlain by the arenaceous and conglomeratic Kurrawang Beds. In the Coolgardie-Norseman area, the stratigraphy is more complicated, but the economically most important unit is the mafic-ultramafic sequence (Gemuts and Theron 1975). Thin black shale and chert units are common throughout the sequence. The top of the sequence is marked by the sulphide-rich »Black chert marker», which consists of jarosite-stained, framboidal chert and black shale. The Ni deposits are situated at the base of the first ultramafic lava sequence just below the »Black chert marker». Most Ni deposits between Coolgardie and Norseman are located or associated with structures of embayments in basalts at the basal contact of serpentinites. In most cases, chert horizons occur along strike from the Ni deposits but are absent in the ore position.

Three ore types are recognised in the Suomussalmi deposits: 1) disseminated ore associated with a vein network in serpentinite, 2) brecciating massive ore in talc—carbonate rocks and in amphibole—chlorite rocks and 3) massive pyrite-rich ore at the base of the serpentinite lens. The host rocks of the ores have been submitted to intense CO_2-metasomatism, hydration and tectonic movements that enriched the primary disseminated ore in the veins and shear zones. Sulphide ore analyses indicate that the massive pyrite-rich ore was generated by reaction between sulphur derived from felsic volcanites and metals liberated during serpentinisation of the ultramafic rocks.

Geochemical whole-rock analyses show that the serpentinites and talc—carbonate rocks in the Suomussalmi deposits are peridotitic (averages 27.76 wt. % and 26.61 wt. % MgO respectively), the amphibole—chlorite rocks are pyroxenitic (averages 17.52 wt. % and 19.20 wt. % MgO respectively) and the coarse-grained amphibolites gabbroic (average 11.09 wt. % MgO and 51.71 wt. % SiO_2). The felsic schists and porphyries are rhyolitic (averages 71.02 wt. % and 70.04 wt. % SiO_2

respectively). The hypabyssal dyke rocks at Peura-aho are granodioritic (averages 61.34 wt. % SiO_2 and 3.72 wt. % MgO); the mafic volcanites are basaltic (average 55.74 wt. % SiO_2 and 8.09 wt. % MgO) or andesitic. As a rock series, the ultramafic and mafic rocks of the Suomussalmi Ni-Cu deposits are predominantly Ca-rich, K-poor, sub-alkalic tholeiitic rocks. The felsic schists, porphyries and black schists are calc-alkalic in composition.

Sulphide ore analyses show characteristic average Cu/(Cu + Ni) ratios of 0.30—0.33. The MgO content of the host rocks in the Suomussalmi deposits is about 20 wt. %, calculated as an average of the serpentinites, talc—carbonate rocks and amphibole—chlorite rocks. Hence, the host rocks in Suomussalmi are transitional in composition between the komatiites of Abitibi and the tholeiites of Pechenga (Naldrett and Cabri 1976). Furthermore, experimental data of Rajamani and Naldrett (1978) suggest that the MgO content calculated for the parental magma in the Suomussalmi deposits might be 8—10 wt. %. If the average Cu/Ni ratios of the Suomussalmi deposits are compared with those of Ni-Cu ores in other Archean greenstone belts in South Africa, Western Australia, Canada and the U.S.S.R., the closest ratios are those from Pechenga, Soviet East Karelia and Canada (Väyrynen 1938, Naldrett and Gasparrini 1971, Ewers and Hudson 1972, Kairjak *et al.* 1976, Naldrett and Cabri 1976, Viljoen *et al.* 1976, Barrett *et al.* 1977, Moeskops and Davis 1977, Naldrett and Turner 1977, Williams 1979 and Naldrett *et al.* 1979).

In the quaternary system Cu-Fe-Ni-S most of the bulk sulphide composition points of Suomussalmi orebodies plot in the area of classical Ni-Cu ores that were formed through magmatic segregation. The pyrite-rich, massive Peura-aho B ore body has an exceptionally high sulphur content and thus indicates sulphurisation. The platinum group elements at Hietaharju are concentrated in the chalcopyrite-rich ore mineral parageneses and at Peura-aho in the massive pyrite-rich ore. The Pt/(Pt+Pd) ratio is transitional between the komatiitic and tholeiitic values (Naldrett and Cabri 1976).

The sulphide mineral parageneses in the Suomussalmi Ni-Cu deposits established by microscope, microprobe and XRD are (Fig. 24):

1) hexagonal pyrrhotite ± troilite + pentlandite + chalcopyrite ± violarite ± pyrite ± cubanite ± mackinawite ± gersdorffite ± sphalerite (Hietaharju A ore);
2) hexagonal ± monoclinic pyrrhotite + pentlandite ± violarite + chalcopyrite ± gersdorffite ± sphalerite (Hietaharju C ore);
3) monoclinic pyrrhotite + pentlandite + chalcopyrite ± pyrite ± violarite ± mackinawite (Peura-aho A ore);
4) monoclinic ± hexagonal pyrrhotite + pyrite + chalcopyrite + violarite ± pentlandite ± sphalerite (Peura-aho B ore).

The oxide ore minerals chromite, magnetite and ilmenite are common in all parageneses. The Zn content in the chromian spinel indicates crystallisation from Zn-bearing sulphide—silicate—oxide liquids. Two modes of origin seem possible for the chromian magnetite rims of the chromites: 1) crystallisation from Fe_3O_4—$FeCr_2O_4$ solid solution depleted in the chromite end member above 900°C or 2) reaction between early formed chromite and magnetite formed during serpentinisation. The Zn-bearing, poorly zoned, Mg-and Al-poor chromites are thought to have crystallised directly from Cr-bearing sulphide melts at low oxygen fugacity. The early formed euhedral magnetites contain drop-shaped inclusions of trapped sulphides. Most of the magnetite grains consist of fine-grained ragged pure Fe_3O_4 that formed as a result of serpentinisation (Fig. 24). Ilmenites crystallised after the magnetite rims of chromites.

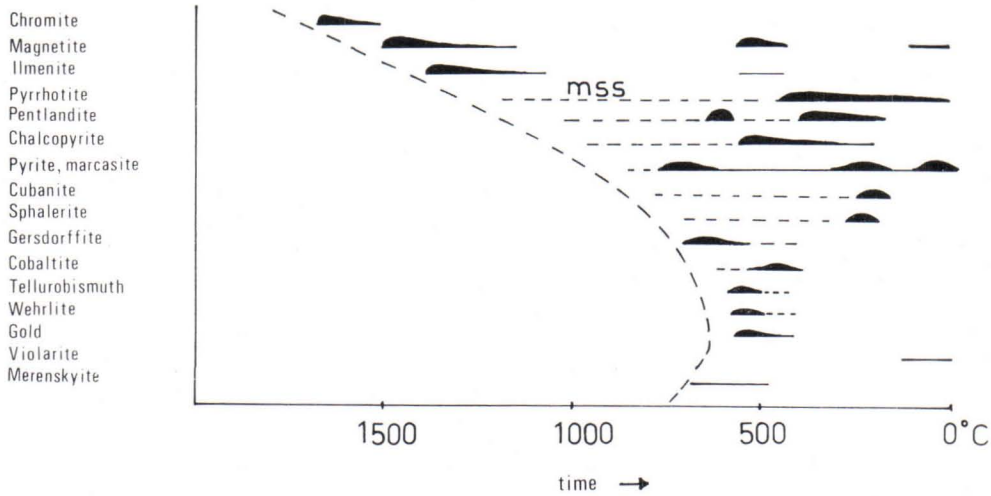

Fig. 24. Paragenetic diagram of the ore minerals in the Suomussalmi Ni-Cu deposits.

Microprobe analysis indicates that hematite and pyrophanite form a solid solution with ilmenite, suggesting rapid crystallisation at above 600°C.

Although some textures in the samples prove that the sulphides were still molten when chromite, magnetite and olivine had already crystallised, the current sulphide mineral parageneses are products of continuous re-equilibration during progressive crystallisation down to low temperatures. The composition and lattice type of pyrrhotite are greatly affected by the original composition of the sulphide melt or solid solution, by the partial pressures of oxygen and sulphur, by the mineral phases exsolved from pyrrhotite solid solution during cooling and by lattice transformations. In an open system, the composition and lattice type of pyrrhotite can change by reacting with circulating iron- and sulphur-bearing solutions (Craig and Scott 1974). Thus, pyrrhotite can hardly be used as a geological thermometer. As is evidenced by the existence of monoclinic pyrrhotite, troilite and mackinawite in the Suomussalmi samples, however, the pyrrhotite-bearing ore mineral parageneses reached their final equilibrium at very low temperatures, less than 254°C.

Pentlandite and violarite are the main Ni- and Co-bearing sulphides (calculated mode from 2.6 to 26.8 wt.%) in the Suomussalmi ore bodies. Pentlandite crystallised as three generations: 1) euhedral pentlandite below 610°C, 2) pentlandite as intergranular bands and 3) lamellar »flame» pentlandite below 400°C, or even below 300°C (Kullerud 1963, Naldrett and Kullerud 1967). At very low temperatures pentlandite was altered through meteoric waters into violarite (Craig and Scott 1974).

Copper is contained almost entirely in chalcopyrite. The twinning observed in chalcopyrite suggests transformation from a cubic intermediate solid solution at 557°C (Craig and Scott 1974). Cubanite that occurs as unusual intergranular rims in the Hietaharju samples is stable below 200—210°C (Cabri *et al.* 1973).

A part of Ni and Co are contained in pyrite which occurs in the Suomussalmi samples as three generations (Fig. 25): 1) Co-bearing euhedral pyrite in the Peura-aho A primary dissemination, 2) Ni-bearing euhedral pyrite

in the Peura-aho B massive ore and 3) secondary pyrite formed through weathering of pyrrhotite. The first generation of pyrite might be of high temperature, less than 743°C (Kullerud and Yoder 1959). Ni-bearing pyrite is associated with the sulphurisation of Fe and Ni released during serpentinisation of the ultramafic rocks. The third generation of pyrite is often intergrown with marcasite, which is stable at low temperatures and is formed through weathering of pyrrhotite (Kullerud 1967, Ramdohr 1975, p. 900).

The minor Zn contents are connected with the copper-rich samples. Sphalerite is in equilibrium with hexagonal and monoclinic pyrrhotite below 250°C (Scott and Kissin 1973). The content of 11.24 mol.% FeS in the analysed sphalerite refers to the mineral pair monoclinic pyrrhotite—sphalerite.

The Ni-Co arsenides are concentrated in the talc—carbonate rock samples of Hietaharju A and C orebodies. This suggests introduction of As in alteration fluids, particularly those enriched in carbonate.

Gersdorffite forms a cubic solid solution with cobaltite at high temperatures. According to the chemical composition of the analysed gersdorffite, the lattice becomes distorted below 500°C (Bayliss 1969). The analysed gersdorffite has a rim of optically anisotropic nickelian cobaltite. The inclusions observed in gersdorffite are gold, tellurobismuthite and wehrlite. The arsenides seem to have acted as collectors for Au, Ag, Te and Bi. Altaite, PbTe, that occurs in chalcopyrite, forms during the later stages of crystallisation. Merenskyite, which is stable below 720°C, is also thought to have formed as a result of reaction between Pd liberated during late magmatic and postmagmatic processes, and Te and Bi which became enriched at later stages of crystallisation (Stumpfl and Tarkian 1976).

Like most Archean Ni-Cu sulphide deposits associated with ultramafic lavas or layered sills, the Suomussalmi Ni-Cu deposits are thought to have formed through magmatic segregation of immiscible sulphide—silicate liquids. The primary disseminated sulphides were later remobilised and concentrated by metamorphism and tectonic activity and to some extent by sulphurisation.

ACKNOWLEDGEMENTS

Much of the present work was carried out at the Institute of Mineralogy and Petrology, University of Heidelberg. I thank Professors G. C. Amstutz, P. Ramdohr and G. Moh for their friendly advice and for allowing me to use the facilities of the Institute.

I am grateful to Professor H. V. Tuominen for permission to use the facilities of the Department of Geology, University of Helsinki, to Professors G. Gaál, K. Rankama and J. Siivola for critically reading the manuscript, and to Dr. M. Lehtinen for assisting with the XRD and calculating problems. I am indebted to Professor Th. G. Sahama for many discussions and for moral support.

I thank Professor H. Papunen, University of Turku, for many fruitful discussions during the work, and Drs. P. Rouhunkoski and A. Häkli, Exploration Department of Outokumpu Oy, for supplying the material for this study and for putting the analytical facilities of the Geological Laboratory of Outokumpu Oy at my disposal.

I gratefully acknowledge the financial aid I received from DAAD (Deutscher Akademischer Austauschdienst), the Foundation for Research of Natural Resources in Finland (Suomen Luonnonvarain Tutkimussäätiö) and Outokumpu Oy.

Mrs. Gillian Häkli checked the language of the manuscript.

I thank Professor L. K. Kauranne, Director of the Geological Survey of Finland, for arranging the publication in the Survey's Bulletin series.

Finally, I express my gratitude to all persons not mentioned by name who contributed in one way or another towards the preparation of this study.

REFERENCES

Arndt, N. T., Naldrett, A. J. & Pyke, D. R., 1977. Komatiitic and iron-rich tholeiitic lavas of Munro Township, Northeast Ontario. J. Petrol. 18, 319—369.

Arndt, N. T., Francis, D. & Hynes, A. J., 1979. The field characteristics and petrology of Archaean and Proterozoic komatiites. Can. Mineral. 17, 147—163.

Arnold, R. G., 1962. Equilibrium relations between pyrrhotite and pyrite from 325° to 743°C. Econ. Geol. 57, 72—90.

— , **1966.** Mixtures of hexagonal and monoclinic pyrrhotite and the measurement of the metal content of pyrrhotite by X-ray diffraction. Am. Mineral. 51, 1221—1227.

Arnold, R. G. & Reichen, Laura, E., 1962. Measurement of the metal content of naturally occuring, metal-deficient, hexagonal pyrrhotite by an X-ray spacing method. Am. Mineral. 47, 105—111.

Arth, J. G., Nicholas, T. & Naldrett, A. J., 1977. Genesis of Archaean komatiites from Munro Township, Ontario: Trace-element evidence. Geology 5, 590—594.

Barrett, F. M., Binns, R. A., Groves, D. J., Marston, R. J. & McQueen, K. G., 1977. Structural history and metamorphic modification of Archean volcanic-type nickel deposits, Yilgarn Block, Western Australia. Econ. Geol. 72, 1195—1223.

Barton, P. B. Jr. & Skinner, B. J., 1967. Sulphide mineral stabilities. *In* Geochemistry of hydrothermal ore deposits, ed. by H. L. Barnes. Holt, Rinehart and Winston, Inc. New York, 236—333.

Barton, P. B., Jr. & Toulmin, P., 1966. Phase relations involving sphalerite in the Fe-Zn-S system. Econ. Geol. 61, 815—849.

Bayliss, P., 1969. X-ray data, optical anisotropism, and thermal stability of cobaltite, gersdorffite, and ullmannite. Mineral. Mag. 37, 26—33.

Blais, S., Auvray, B., Bertrand, J. M., Capdevila, R., Hameurt, J. & Vidal, P., 1977. Les grands traits géologiques de la ceinture archéenne de roches vertes de Suomussalmi-Kuhmo (Finland orientale). Bull. Soc. géol. France 1977, 7. ser, 19 (5), 1033–1039.

Blais, S., Auvray, B., Capdevila, R., Jahn, B. M., Hameurt, J. & Bertrand, J. M., 1978. The Archaean greenstone belts of Karelia (eastern Finland) and their komatiitic and tholeiitic series. *In* Archaean geochemistry, ed. by B. F. Windley and S. M. Naqvi, Elsevier, 87—107.

Brooks, C. & Hart, S. R., 1974. On the significance of komatiite. Geology 2, 107—110.

Burgmann, W. Jr., Urbain, G. & Frohberg, M. G., 1968. Contribution a l'étude du système fer-soufre limité au domaine du mono-sulfure de fer (pyrrhotine). Mem. Sci. Rev. Métall. 65, 567—578.

Cabri, J. L., 1973. New data on phase relations in the Cu-Fe-S system. Econ. Geol. 68, 443—454.

Cabri, J. L., Szymanski, J. T. & Stewart, J. M., 1973. On the transformation of cubanite. Can. Miner. 12, 33—38.

Craig, J. R., 1971. Violarite stability relations. Am. Mineral. 56, 1303—1311.

Craig, J. R. & Kullerud, G., 1969. Phase relations in the Cu-Fe-Ni-S system and their application to magmatic ore deposits. Econ. Geol. Monogr. 4, 344—358.

Craig, J. R. & Scott, S. D., 1974. Sulfide phase equilibria. *In* Sulfide mineralogy. Mineralogical Society of America, Short Course Notes, V. 1, ed. by P. H. Ribbe, CS 1—110.

Cremer, V., 1969. Mischkristallbildung in System Chromit-Magnetit-Hercynit zwischen 1000°C and 500°C. Neues Jahrb. Mineral. Abh. 111, 184—205.

Czamanske, G. K., Himmelberg, G. R. & Goff, F. E., 1976. Zoned Cr, Fe-spinel from the La Perouse layered gabbro, Fairweather Range, Alaska. Earth and Planet. Sci. Lett. 33, 111—118.

Deer, W. A., Howie, R. A. & Zussmann, J., 1962. Rock forming minerals. Vol. 5. Longmans, Green and Co Ltd, London. 371 p.

El Goresy, A. & Kullerud, G., 1969. The Cr-S and Fe-Cr-S systems. Carnegie Inst. Wash., Year Book 67, 182—187.

Evans, B. W. & Frost, B. R., 1975. Chrome-spinel in progressive metamorphism - a preliminary analysis. Geochim. Cosmochim. Acta 39, 959—972.

Ewers, W. E. & Hudson, D .R., 1972. An interpretative study of a nickel-iron sulfide ore intersection, Lunnon Shoot, Kambalda, Western Australia. Econ. Geol. 1075—1092.

Gaál, G., Mikkola, A. & Söderholm, B., 1978. Evolution of the Archaean crust in Finland. Precambrian Res. 6, 199—215.

Gee, R. D., 1975. Regional geology of the Archaean nucleii of the Western Australia. *In* Economic geology of Australia and Papua New Guinea. 1. Metals, ed. by C. L. Knight. Australasian Inst. of Mining and Metallurgy, Monogr. 5., 43—55.

Gemuts, I. & Theron, A., 1975. The Archaean between Coolgardie and Norseman — stratigraphy and mineralization. *In* Economic geology of Australia and Papua New Guinea. 1. Metals, ed. by C. L. Knight. Australasian Inst. of Mining and Metallurgy, Monogr. 5., 66—74.

Green, D. H., Nicholls, J. A., Viljoen, M. & Viljoen, R., 1974. Experimental demonstration of the existence of peridotitic liquids in earliest Archaean magmatism. Geology 3 (1), 11—14.

Groves, D. J., Barrett, F. M., Binns, R. A. & McQueen, K. G., 1977. Spinel phases associated with metamorphosed volcanic-type iron-nickel sulfide ores from Western Australia. Econ. Geol. 72, 1224—1244.

Haapala, P. S., 1969. Fennoscandian nickel deposits. Econ. Geol. Mon. 4, 262—275.

Haggerty, S. E., 1976. Opaque mineral oxides in terrestrial igneous rocks. *In* Oxide minerals. Mineralogical Society of America, Short Course Notes, V. 3, ed. by D. Rumble III, Hg 101—300.

Hawley, I. E. 1962. The Sudbury ores: Their mineralogy and origin. Can Mineral. 7 (1), 207 p.

Henry, N. F. M. (Editor), 1977. IMA/COM Quantitative Data File, First Issue. McCrone Research Associates Ltd., London.

Hoffman, E. & MacLean, W. H., 1976. Phase relations of michenerite and merenskyite in the Pd-Bi-Te system. Econ. Geol. 71, 1461—1468.

Huhma, M., 1978. Elohopeatutkimus I. Mustaliuskeet [Mercury project I. Black shales] Unpub. report, Outokumpu Oy, Exploration Department.

Inkinen, O., 1970 a. Suomussalmen Hietaharjun ja Peura-ahon Ni-malmiaiheiden tutkimukset 1969···1970 [The exploration of the Ni prospects at Hietaharju and Peura-aho in Suomussalmi 1969—1970]. Unpub. report, Outokumpu Oy, Exploration Department.

— , **1970 b.** Suomussalmen Peura-ahon malmiaiheen jatkotutkimukset kesällä 1970 [The continued exploration at the Peura-aho prospect in Suomussalmi, summer 1970]. Unpub. report, Outokumpu Oy, Exploration Department.

Irvine, T. N., 1965. Chromian spinel as petrogenetic indicator, I. Theory. Can. J. Earth Sci. 2, 648.

Irvine, T. N & Baragar, R. A., 1971. A guide to the chemical classification of the common volcanic rocks. Can. J. Earth. Sci. 8, 523—548.

Kairjak, A. I., Morozov, S. A., Limonova, L. P. & Popov, M. G., 1976. Itäisen Karjalan Cu-, Ni- ja polymetallikiisuaiheet [The Cu-Ni and polymetallic prospects in eastern Karelia]. Razvedka i ohrana nedr 1976 (8), 2—7. (Translation from Russian to Finnish, translation collection of the Exploration Dept. of Outokumpu Oy.)

Kingston, G. A., 1966. The occurrence of platinoid bismuthotellurides in the Merensky Reef at Rustenburg platinum mine in Western Bushveld. Mineral. Mag. 35, 813—834.

Kissin, S. A., 1974. Phase relations in a portion of the Fe-S system. Ph.D. thesis, University of Toronto, Canada.

Knight, C. L. (Editor), 1975. Economic geology of Australia and Papua New Guinea. 1. Metals. Australasian Inst. of Mining and Metallurgy Monogr. 5. 1126 p.

Knop, O., Ibrahim, M. A. & Sutarno, 1965. Chalcogenides of transition elements. IV. Pentlandite, a natural π-phase. Can. Mineral. 8, 291—316.

Kojonen, K. K., 1974. Heksagoninen ja monokliininen pyrrotiitti Vuonoksen, Luikonlahden ja Outokummun malmeissa [Hexagonal and monoclinic pyrrhotite in the ores of Vuonos, Luikonlahti and Outokumpu]. Unpub. M.Sc. thesis, Dept. of Geology, Univ. of Helsinki.

— , **1976.** Experiments on synthetic pentlandite. *In* Ore mineral systems, ed. by G. H. Moh. N. Jb. Mineral., Abh. 126, (2), 126—145.

Kokkola, M., 1968. Kiannan alueen vulkaanisesta muodostumasta [On the volcanogenic formation of Kianta area]. Unpub. M. Sc. thesis, Dept. of Geology, Univ. of Turku.

Kouvo, O., 1958. Radioactive age of some Finnish

pre-Cambrian minerals. Bull. Comm. géol. Finlande 182. 70 p.

Kouvo, O. & Tilton, F. R., 1966. Mineral ages from the Finnish Precambrian. J. Geol. 74, 421—442.

Kouvo, O., Huhma, M. & Vuorelainen, Y., 1959. A natural cobalt analogue of pentlandite. Am. Mineral., 44, 897—900.

Kullerud, G., 1963. Thermal stability of pentlandite. Can. Mineral., 7, 353—366.

— , 1967. Sulfide studies. *In* Research in geochemistry. Vol. 2, ed. by P. H. Abelson, John Wiley and Sons, 286—321.

— , 1968. Sulfide phase equilibria and their application to ores. Lectures. Lehigh University. 264 p.

Kullerud, G. & Yoder, H. S., 1959. Pyrite stability relations in the Fe-S system. Econ. Geol. 54, 533—572.

Kullerud, G., Yund, R. A. & Moh, G. H. 1969. Phase relations in the Cu-Fe-S, Cu-Ni-S and Fe-Ni-S systems. Econ. Geol. Monogr. 4, 323—343.

Kuznetsov, V. G., Sokolova, M. A., Palkina, K. K. & Popova, Z. V., 1965. The cobalt-sulphur system. Izv. Akad. Nauk. SSSR, Neorgan. Materialy 1 (5), 675—689. (English transl., Russ. J. Inorgan Materials 1966, 617—632).

Lindsley, D. H., 1976. The crystal chemistry and structure of oxide minerals as exemplified by the Fe-Ti-oxides *In* Oxide Minerals. Mineralogical Society of America, Short Course Notes, V. 3, ed. by D. Rumble, L 1—60.

Matisto, A., 1958. Kivilajikartan selitys D 5, Suomussalmi. English summary. General geological map of Finland 1 : 400 000. 115 p.

Middlemost, E. A. K., 1975. The basalt clan. Earth-Sci. Rev. 11, 337—364.

Moeskops, P. G. & Davis, G. R., 1977. Unusual sulphide replacement textures in altered olivine-rich rocks of the Bulong Complex near Kalgoorlie, Western Australia. Mineral. Mag. 41, 473—479.

Morimoto, N. & Kullerud, G., 1964. Pentlandite: Thermal expansion. Carnegie Inst. Wash. Year Book 63, 204—205.

Muir, T. L., 1979. Discrimination between extrusive and intrusive Archaean ultramafic rocks in the Shaw Dome area using selected major and trace elements. Can. J. Earth. Sci. 16, 80—90.

Mutanen, T., 1976. Komatiites and komatiite provinces in Finland. Geologi 28 (4—5), 49—56.

Naldrett, A. J., 1969. A portion of the system Fe-S-O between 900° and 1080°C and its application to sulfide ore magmas. J. Petrol. 10 (2), 171—201.

Naldrett, A. J. & Cabri, L. I., 1976. Ultramafic and related mafic rocks: Their classification and genesis with special reference to the concentration of nickel sulfides and platinum-group elements. Econ. Geol. 71, 1131—1158.

Naldrett, A. J. & Gasparrini, E. L., 1971. Archaean nickel sulphide deposits in Canada: Their classification, geological setting and genesis with some suggestions as to exploration. Spec. Publs. Geol. Soc. Aust. 3, 201—226.

Naldrett, A. J. & Kullerud, G., 1967. A study of the Strathcona Mine and its bearing on the origin of the nickel-copper ores of the Sudbury district, Ontario. J. Petrol. 8 (3), 453—531.

Naldrett, A. J. & Turner A. R., 1977. The geology and petrogenesis of a greenstone belt and related nickel sulfide mineralization at Yakabindie, Western Australia. Precambrian Res. 5, 43—103.

Naldrett, A. J., Craig, J. R. & Kullerud, G., 1967. The central portion of the Fe-Ni-S system and its bearing on pentlandite solution in iron-nickel ores. Econ. Geol. 62, 826—847.

Naldrett, A. J., Hoffman, E. L., Green, A. H., Chen-Lin Chou & Naldrett, S. R., 1979. The composition of Ni-sulfide ores, with particular reference to their content of PGE and Au. Can. Mineral. 17, 403—415.

Nesbitt, R. W., 1971. Skeletal crystal forms in the ultramafic rocks of the Yilgarn block, Western Ausralia: Evidence for an Archaean ultramafic liquid. Spec. Publs. geol. Soc. Aust. 3, 331—347.

Nesbitt, R. W. & Sun, Shen-Su, 1976. Geochemistry of Archaean spinifex-textured peridotites and magnesian and low-magnesian tholeiites. Earth and Planet. Sci. Lett. 31, 433—453.

Nesbitt, R. W., Sun, Shen-Su & Purvis, A. C., 1979. Komatiites: Geochemistry and genesis. Can. Mineral. 17, 165—186.

Papunen, H., 1970. Sulfide mineralogy of the Kotalahti and Hitura nickel-copper ores, Finland. Ann. Acad. Sci. Fennicae. Ser. A, No. 109. 74 p.

Papunen, H., Idman, H., Neuvonen, K. J., Pihlaja, P. & Talvitie, J., 1977. Lapin ultramafiiteista. Summary: The ultramafics in Lapland. Geological Survey of Finland, Rep. Invest. no. 23. 87 p.

Papunen, H., Häkli, T. A. & Idman, H., 1979. Geological, geochemical and mineralogical features of sulfide-bearing ultramafic rocks in Finland. Can. Mineral. 17, 217—232.

Pehkonen, E., 1963. Suomussalmen Kiannanniemen tutkimuksista [On the exploration at Kiannanniemi in Suomussalmi]. Unpub. report, Outokumpu Oy, Exploration Department.

Power, L. F. & Fine, H. A., 1976. The iron-sulphur system. Minerals Sci. Engng. 8 (2), 106—128.

Rajamani, V. & Naldrett, A. J., 1978. Partitioning of Fe, Co, Ni and Cu between sulfide liquid and basaltic melts and the composition of Ni-Cu sulfide deposits. Econ. Geol. 73, 82—93.

Ramdohr, P., 1969. The ore minerals and their intergrowths. Pergamon Press, Oxford. 1174 p.

—, 1975. Die Erzmineralien und ihre Verwachsungen. Akademie-Verlag, Berlin. 1277 p.

Rankama, K., 1954. Origin of carbon in some early Precambrian carbonaceous slates from southeastern Manitoba, Canada. Bull. Comm. géol. Finlande 166, 5—20.

Rantala, E., 1963. Suomussalmen pitäjän Kiannan-Saarijärven suprakrustisen muodostuman pohjoisosan vulkanogeenisista kivilajeista [On the volcanogenic rock types of the supracrustal formation of the Kianta-Saarijärvi area, commune of Suomussalmi]. Unpub. M.Sc. thesis. Dept. of Geology, Univ. of Helsinki.

Rising, B. A., 1973. Phase relations among pyrite, marcasite and pyrrhotite below 300°C. Ph.D. thesis, Pennsylvania State University, University Park, Pennsylvania.

Schneiderhöhn, H., 1952. Erzmikroskopisches Praktikum, E. Schweizerbartsche Verlagsbuchhandlung (Erwin Nägele), Stuttgart. 274 p.

Schott, E. H., Ottemann, J. & Omenetto, P., 1972. Some new observations on mackinawite and valleriite. Rend. Soc. Ital. Mineral. Petrol. 28, 241—295.

Scott, S. D. & Barnes, H. L., 1971. Sphalerite geothermometry and barometry. Econ. Geol. 66, 653—669.

Scott, S. D. & Kissin, S. A., 1973. Sphalerite composition in the Zn-Fe-S system below 300°C. Econ. Geol. 68, 475—479.

Simonen, A. 1971. Das finnische Grundgebirge. Geol. Rundschau 60 (4), 1406—1421.

Simpson, P. R., Lopez Soler, A. & Cope, M. J., 1977. Chromite, card number 1.600. *In* IMA/COM Quantitative Data File, ed. by N. F. M. Henry.

Srivastava, R. K., 1977. A comprehensive atomic absorption and spectrophotometric scheme for the determination of major and trace elements in rocks and minerals. N. Jb. Mineral. Mh. 9, 425—432.

Stumpfl, E. F. & Tarkian, M., 1976. Platinum genesis: New mineralogical evidence. Econ. Geol. 71, 1451—1460.

Takeno, S. & Clark, A. H., 1967. Observations on tetragonal (Fe, Ni, Co)$_{1+x}$S, mackinawite. J. Sci. Hiroshima Univ., Ser. C, 5, 287—293.

Thayer, T. P., Milton, C., Dinnin, J. & Rose, H. Jr., 1964. Zincian chromite from Outokumpu, Finland. Am. Mineral. 49, 1178—1183.

Toulmin, P. & Barton, P. B. Jr., 1964. A thermodynamic study of pyrite and pyrrhotite. Geochim. Cosmochim. Acta 28, 641—671.

Vaasjoki, O., Häkli, T. A. & Tontti, M., 1974. The effect of cobalt on the thermal stability of pentlandite. Econ. Geol. 69, 549—551.

Vaughan, D. J., 1969. Nickelian mackinawite from Vlakfontein, Transvaal. Am. Mineral. 54, 1190—1193.

Vaughan, D. J. & Craig, J. R., 1978. Mineral chemistry of metal sulfides. Cambridge University Press. 493 p.

Väyrynen, H., 1938. Petrologie des Nickelerzfeldes Kaulatunturi-Kammikivitunturi in Petsamo. Bull. Comm. géol. Finlande, 116, 198 p.

Viljoen, M. J. & Viljoen, R. P., 1969 a. An introduction to the geology of the Barberton granite-greenstone terrain. Upper Mantle Project. Spec. Publs. Geol. Soc. S. Afr. 2, 9—28.

Viljoen, M. J. & Viljoen, R. P., 1969 b. The geology and geochemistry of the lower ultramafic unit of the Onverwacht Group and a proposed new class of igneous rocks. Upper Mantle Project. Spec. Publs. Geol. Soc. S. Afr. 2, 55—86.

Viljoen, M. J. & Viljoen, R. P., 1969 c. Evidence for the existence of a mobile extrusive peridotitic magma from Komati Formation of the Onverwacht Group. Upper Mantle Project. Spec. Publs. Geol. Soc. S. Afr. 2, 87—123.

Viljoen, M. J. & Viljoen, R. P., 1969 d. A proposed new classification of the granitic rocks of the Barberton region. Upper Mantle Project. Spec. Publs. Geol. Soc. S. Afr. 2, 153—188.

Viljoen, M. J., Bernasconi, A., van Coller, N., Kinloch, E. & Viljoen, R. P., 1976. The geology of the Shangani Nickel Deposit, Rhodesia. Econ. Geol. 71, 76—95.

Vogt, J. H. L., 1893. Bildung von Erzlagerstätten durch Differentationsprozesse im basischen Eruptivmagmata. Z. prakt. Geol. 4—11, 125—143, 257—284.

— , 1917. Die Sulfid-Silikat-Schmelzlösungen. Norsk. Geol. Tidskr. 4, 151—247.

Wetherill, G. H., Kouvo, O., Tilton, G. R. & Gast, P. W. 1962. Age measurements on rocks from the Finnish Precambrian. J. Geol. 70, 74—88.

Wiik, B., 1953. Composition and origin of soapstone. Bull. Comm. géol. Finlande 165. 57 p.

Williams, D. A. C., 1979. The association of some nickel sulfide deposits with komatiitic volcanism in Rhodesia. Can. Mineral. 17, 337—349.

Winkler, H. G. F., 1976. Petrogenesis of metamorphic rocks. Fourth edition. Springer Verlag. 334 p.

Tätä julkaisua myy

VALTION PAINATUSKESKUS
MARKKINOINTIOSASTO

Postimyynti
PL 516
00101 HELSINKI 10
Puh. 90-539 011

Kirjakauppa
Annankatu 44
00100 HELSINKI 10
Puh. 90-17341

Denna publikation säljes av

STATENS TRYCKERICENTRAL
MARKNADSFÖRENINGSAVDELNINGEN

Postförsäljning
PB 516
00101 HELSINGFORS 10
Tel. 90-539 011

Bokhandel
Annegatan 44
00100 HELSINGFORS 10
Tel. 90-17341

This publication can be obtained from

GOVERNMENT PRINTING CENTRE
MARKETING DEPARTMENT

Bookshop
Annankatu 44
00100 HELSINKI 10
Phone 90-17341

Orders from abroad:
AKATEEMINEN KIRJAKAUPPA
Keskuskatu 1
SF-00100 Helsinki 10

ISBN 951-690-138-7
ISSN 0367-522X